Electronic Supplementary Material (ESI) for Nanoscale.

Supporting Information

Triptycene Molecular Rotor Mounted on Metallofullerene $Sc_3C_2@C_{80}$ and Their Spin-Rotation Couplings

*Haibing Meng[a,b], Chong Zhao[a,b], Mingzhe Nie[a,b], Chunru Wang[*a] and Taishan Wang[*a]*

[a]Beijing National Laboratory for Molecular Sciences, Key Laboratory of Molecular Nanostructure and Nanotechnology, Institute of Chemistry, Chinese Academy of Sciences, Beijing 100190, China

[b]University of Chinese Academy of Sciences, Beijing 100049, China

*E-mail: wangtais@iccas.ac.cn; crwang@iccas.ac.cn

Table of Contents

Materials and methods

Unless otherwise noted, all solvents and reagents were obtained from commercial sources and used without further purification. The $Sc_3C_2@C_{80}$ was synthesized according to the literature.[1, 2] All NMR spectra were performed on a Bruker AVANCE III-500 (500 MHz) spectrometer using chloroform-d ($CDCl_3$) and 1,1,2,2-tetrachloroethane-d_2 ($CD_2Cl_2CD_2Cl_2$) as the solvents. Chemical shifts are reported in ppm relative to tetramethylsilane (0 ppm) for ^{1}H and ^{13}C NMR measurements. Abbreviations: s, singlet; d, doublet; t: triplet; m: multiplet, dd: doublet of doublets, and dq, doublet of quartets. All mass data (EI, MALDI) were recorded on SHIMADZU QP2010 and Bruker Autoflex III mass spectrometers. IR spectra were recorded on Thermo Fisher iN10-iZ10 infrared microspectrography. Melting points were performed on SRS MPA100. The C_{60} and $Sc_3C_2@C_{80}$ derivatives were isolated and purified by high performance liquid chromatography (HPLC) with 20×250 mm Buckyprep column.

The EPR spectra were measured on Bruker E500 with continues-wave X band frequency (~9.5 GHz). For all EPR experiments, 10 mW microwave power was used and EPR signal saturation was avoided. In addition, all the spectra were recorded in the atmosphere of Ar. The strength and frequency of the modulating field were respectively 2 G and 100 kHz. The temperature was controlled by digital

temperature control systems ER4131VT with liquid gaseous nitrogen. The simulations of EPR spectra were performed using EasySpin simulation package implemented in Matlab.[3]

Synthesis of 6, 7, 8, 9, 10, 11, 12

Synthesis of 4-(anthracen-9-yl)benzaldehyde (4)

A round-bottom flask was charged with 4-bromobenzaldehyde (**2)** (185mg, 1 mmol, 1.0 eq), anthracen-9-ylboronic acid (**1)** (222 mg, 1 mmol, 1.0 eq), K_2CO_3 (828 mg, 6 mmol, 6 eq), 5% tetrakis(triphenylphosphine)palladium (0) (58 mg, 0.05 mmol, 0.05 eq), H_2O (2.5 mL) and toluene (20 mL). After three vacuum/argon cycles to remove air from the reaction flask, the reaction mixture was refluxed under argon for 24 h. Then the mixture was diluted with H_2O (10 mL) and extracted with AcOEt for three times. The obtained organic layers were washed with brine (10 mL) and dried (Na_2SO_4) and then concentrated under reduced pressure. Compound **4** was purified by silica gel column chromatography (hexanes/ethyl acetate = 9/1) to give the product as a yellow solid (253.8 mg, 90%).

^{1}H NMR (400 MHz, $CDCl_3$, 298 K) δ 10.20 (s, 1H), 8.54 (s, 1H), 8.15-8.04 (m, 4H), 7.67-7.60 (m, 2H), 7.57 (d, *J* = 8.8 Hz, 2H), 7.48 (dd, *J* = 8.4, 6.6 Hz, 2H), 7.42-7.31 (m, 2H); ^{13}C NMR (101 MHz, $CDCl_3$, 298 K) δ 192.02, 145.81, 135.69, 135.25, 132.14, 131.29, 129.80, 129.79, 128.53, 127.37, 126.16, 125.87, 125.27; mp : 162-164 ℃； IR : 3054 (C-H), 2842 (C-H), 1700 (C=O), 1650 (ar), 1558 (ar), 1538 (ar), 1519 (ar) cm^{-1}; MS (EI) m/z (100%): 282 (100) [M$^+$], 253 (49) [M$^+$-CHO].

Synthesis of 4-(anthracen-9-yl)-3-methylbenzaldehyde (5)

The reaction was carried out as described in the synthesis of **4** using 4-bromo-3-methylbenzaldehyde (**3**) (199.5 mg, 1 mmol, 1.0 eq), affording compound **5** as a light yellow solid (222mg, 75%). This product was also purified by silica gel column chromatography (hexanes/ethyl acetate = 9/1).

^{1}H NMR (400 MHz, $CDCl_3$, 298 K) δ 10.16 (s, 1H), 8.54 (s, 1H), 8.08 (d, *J* = 8.5 Hz, 2H), 7.98 (s, 1H), 7.91 (d, *J* = 7.6 Hz, 1H), 7.57-7.44 (m, 3H), 7.44-7.32 (m, 4H), 1.95 (s, 3H); ^{13}C NMR (101 MHz, $CDCl_3$, 298 K) δ 192.30, 145.35, 139.22, 136.18, 134.63, 132.10, 131.36, 131.12, 129.42, 128.63, 127.85, 127.45,

127.09, 125.96, 125.79, 125.28, 123.77, 19.63; mp : 172-175 ℃； IR : 3054 (C-H), 2950 (C-H), 2919 (C-H), 2831 (C-H), 2723 (C-H), 1700 (C=O), 1623 (ar), 1600 (ar), 1565 (ar), 1519 (ar), 1442 (C-H), 744 (C-H) cm^{-1}; MS (EI) m/z (100%): 296 (100) [M^+], 267 (20) [M^+-CHO].

Synthesis of 4-(9, 10-[1, 2]benzenoanthracen-9(10H)-yl)benzaldehyde (6)

A solution of **4** (282 mg, 1 mmol, 1.0 eq) in 1,2-dimethoxyethane (DME) (5 mL) was heated to reflux while stirring. Both solutions of anthranilic acid (2.74 g, 20 mmol, 20.0 eq) in DME (8 mL) and isopropyl nitrite (2.34 g, 20 mmol, 20.0 eq) in DME (10 mL) were added simultaneously and at the same rate over 3 h by a double syringe pump. After the addition of reagents, the reaction mixture was refluxed for an additional 16 h. The obtained mixture was concentrated and subjected to column chromatography (hexanes/dichloromethane = 6/1) to give **6** as a white solid (71.6 mg, 20%).

^{1}H NMR (500 MHz, $CDCl_2CDCl_2$, 298 K) δ 10.16 (s, 1H), 8.28 (d, *J* = 8.0 Hz, 2H), 8.14 (d, *J* = 7.9 Hz, 2H), 7.45 (d, *J* = 7.2 Hz, 3H), 7.17 (d, *J* = 7.8 Hz, 3H), 7.04 (t, *J* = 7.4 Hz, 3H), 6.97 (t, *J* = 7.6 Hz, 3H), 5.44 (s, 1H); ^{13}C NMR (126 MHz, $CDCl_2CDCl_2$, 298 K) δ 192.34, 146.53, 145.94, 143.38, 135.18, 132.13, 129.82, 125.51, 124.90, 124.35, 124.12, 60.41, 54.87; mp : 193-195 ℃; IR : 3070 (C-H), 2954 (C-H), 2923 (C-H), 2854 (C-H), 2757 (C-H), 2730 (C-H), 1704 (C=O), 1604 (ar), 1581 (ar), 1504 (ar), 1454 (ar), 1442 (ar) cm^{-1}; MS (EI) m/z (100%): 358 (100) [M^+], 329 (45) [M^+-CHO].

Synthesis of 4-(9,10-[1,2]benzenoanthracen-9(10H)-yl)-3-methylbenzaldehyde (**7**)

The reaction was carried out as described in the synthesis of **6** using 4-(anthracen-9-yl)-3-methylbenzaldehyde (**5**) (296 mg, 1 mmol, 1.0 eq), affording compound **7** as a light yellow solid (37.2mg, 10%). This compound was purified by silica gel column chromatography (hexanes/dichloromethane = 4/1).

^{1}H NMR (500 MHz, $CDCl_2CDCl_2$, 378 K) δ 10.19 (s, 1H), 8.69 (d, *J* = 8.2 Hz, 1H), 8.01-7.94 (m, 2H), 7.43 (d, *J* = 7.1 Hz, 3H), 7.18 (d, *J* = 7.5 Hz, 3H), 7.02 (t, *J* = 7.3 Hz, 3H), 6.95 (t, *J* = 7.5 Hz, 3H), 5.36 (s, 1H), 1.90 (s, 3H); ^{13}C NMR (126 MHz, $CDCl_2CDCl_2$, 298 K) δ 192.61, 145.51, 143.07, 141.33, 135.20, 134.02, 131.50, 126.88, 124.82, 124.76, 123.98, 60.50, 54.97, 25.67; mp : 206-208 ℃; IR : 3066 (C-H), 2958 (C-

H), 2923 (C-H), 2834 (C-H), 2811 (C-H), 2723 (C-H), 1700 (C=O), 1600 (ar), 1577 (ar), 1562 (ar), 1488 (ar), 1457 (ar), 1415 (C-H), 752 (C-H) cm^{-1}; MS (EI) m/z (100%): 372 (100) [M^+], 343 (45) [M^+-CHO].

Synthesis of compound 8

C_{60} was heated under argon with N-ethylglycine and compound **6** at 120 ℃ to give compound **8** with yields of nearly 10% in toluene solution for 1 h. After cooling to room temperature, the pure **8** was isolated and purified by high performance liquid chromatography (HPLC) with 20×250 mm Buckyprep column (flow rate: 6 ml/min).

^{1}H NMR (500 MHz, $CDCl_2CDCl_2$, 378 K) δ 8.16 (d, *J* = 8.1 Hz, 2H), 8.09 (d, *J* = 8.2 Hz, 2H), 7.34 (d, *J* = 7.2 Hz, 3H), 7.13 (d, *J* = 7.7 Hz, 3H), 6.93 (t, *J* = 7.3 Hz, 3H), 6.84 (t, *J* = 7.5 Hz, 3H), 5.30 (d, *J* = 6.1 Hz, 2H), 5.17 (d, *J* = 9.2 Hz, 1H), 4.32 (d, *J* = 9.3 Hz, 1H), 3.61 (dq, *J* = 14.6, 7.4 Hz, 1H), 2.91 (dq, *J* = 12.8, 6.7 Hz, 1H), 1.61 (t, *J* = 7.1 Hz, 3H); ^{13}C NMR (126 MHz, $CDCl_2CDCl_2$, 298 K) δ 147.28, 146.60, 146.24, 145.90, 145.56, 145.28, 144.62, 143.15, 142.54, 142.15, 142.00, 141.72, 140.09, 136.85, 125.21, 124.61, 123.93, 81.65, 54.86, 47.37, 29.79, 13.61; mp : ＞ 280℃; IR : 3062 (C-H), 2958 (C-H), 2923 (C-H), 2850 (C-H), 2796 (C-H), 2225 (C=C), 1635 (ar), 1608 (ar), 1542 (ar), 1508 (ar), 1454 (ar), 1430 (C-C), 1380 (C-H), 1288 (C-H), 1187 (C-C), 806 (C-H), 744 (C-H), 682 (C-C) cm^{-1}; MS (MALDI) m/z (100%): 1121 (100) [M^+].

Synthesis of compound 9

C_{60} was heated under argon with N-ethylglycine and compound **7** at 120 ℃ to give compound **9** with yields of nearly 60% in toluene solution for 3 h. The purification of **9** was also the same as that of **8**.

^{1}H NMR (500 MHz, $CDCl_2CDCl_2$, 378 K) δ 8.53 (d, *J* = 8.3 Hz, 1H), 7.93 (d, *J* = 8.3 Hz, 1H), 7.88 (s, 1H), 7.32 (d, *J* = 7.2 Hz, 3H), 7.08 (d, *J* = 7.7 Hz, 3H), 6.92 (t, *J* = 7.3 Hz, 3H), 6.83 (t, *J* = 7.6 Hz, 3H), 5.26 (s, 2H), 5.16 (d, *J* = 9.2 Hz, 1H), 4.31 (d, *J* = 9.3 Hz, 1H), 3.64 (dq, *J* = 14.5, 7.4 Hz, 1H), 2.92 (dq, *J* = 13.8, 7.1 Hz, 1H), 1.72 (s, 3H), 1.61 (t, *J* = 7.2 Hz, 3H); ^{13}C NMR (126 MHz, $CDCl_2CDCl_2$, 298 K) δ 156.73, 154.30, 153.93, 153.55, 147.27, 146.89, 146.60, 146.24, 146.11, 146.04, 145.88, 145.54, 145.23, 145.09, 144.68, 144.33, 143.16, 142.97, 142.64, 142.52, 142.27, 142.13, 141.99, 141.68, 141.62, 140.16,

140.04, 139.79, 138.90, 136.68, 135.98, 135.83, 128.36, 125.04, 124.59, 123.78, 81.41, 68.87, 66.52, 54.98, 47.37, 25.88, 13.62; mp : ＞ 280℃; IR : 3062 (C-H), 2966 (C-H), 2923 (C-H), 2869 (C-H), 2850 (C-H), 2792 (C-H), 2225 (C=C), 1673 (ar), 1608 (ar), 1542 (ar), 1508 (ar), 1454 (ar), 1430 (C-C), 1380 (C-H), 1349 (C-H), 1288 (C-H), 1187 (C-C), 748 (C-H), 701 (C-C) cm^{-1}; MS (MALDI) m/z (100%): 1134 (100) [M^+].

Synthesis of compound 10

$Sc_3C_2@C_{80}$ was heated under argon with N-ethylglycine and compound **6** at 120 ℃ to give compound **10** with yields of nearly 30% in toluene solution for 30 min. After cooling to room temperature, the pure **10** was isolated and purified by high performance liquid chromatography (HPLC) with 20×250 mm Buckyprep column (flow rate: 12 ml/min).

Synthesis of compound 11 and 12

The reaction was carried out as described in the synthesis of **10** using **7**, affording compound **11** (yield: about 40%). The isolation of it was the same as that of **10**. The compound **12** was also obtained through the same reaction of N-ethylglycine, benzaldehyde and $Sc_3C_2@C_{80}$ and isolated by HPLC.

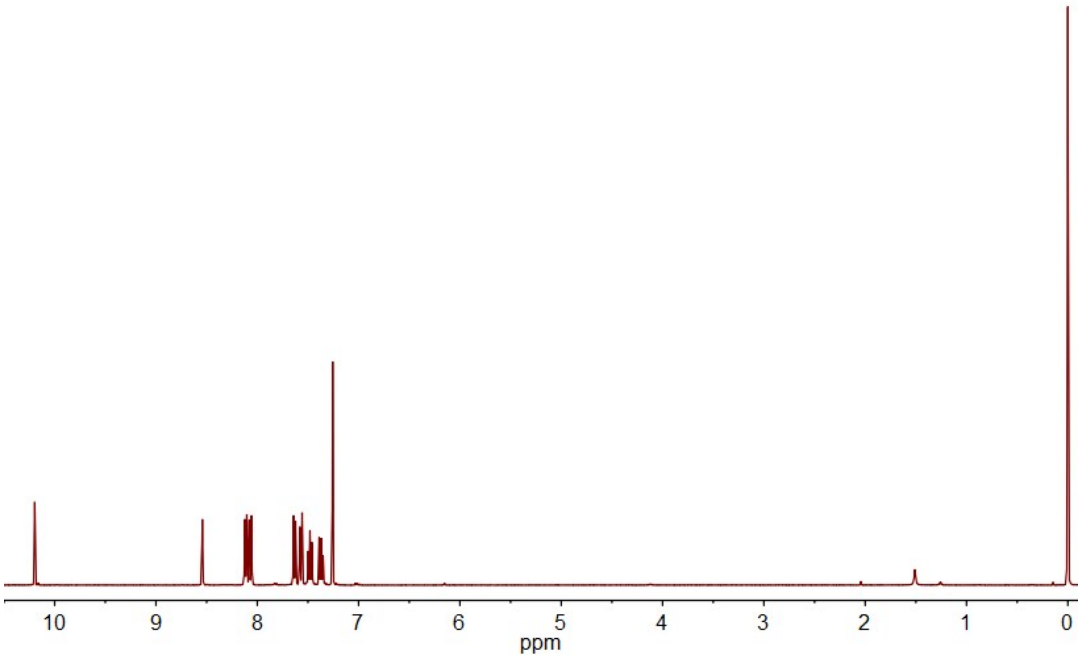

Figure S1. 1H NMR spectrum of 4 (CDCl3, 400 MHz, 298 K)

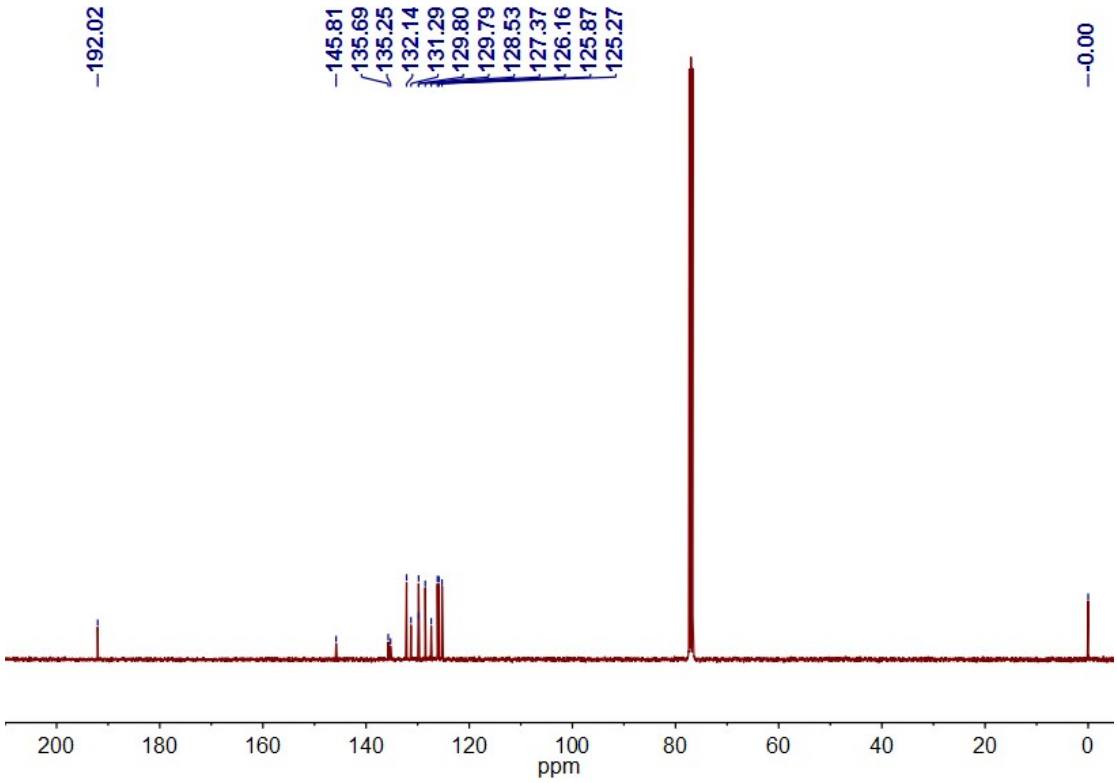

Figure S2. ^{13}C NMR spectrum of **4** ($CDCl_3$, 101 MHz, 298 K)

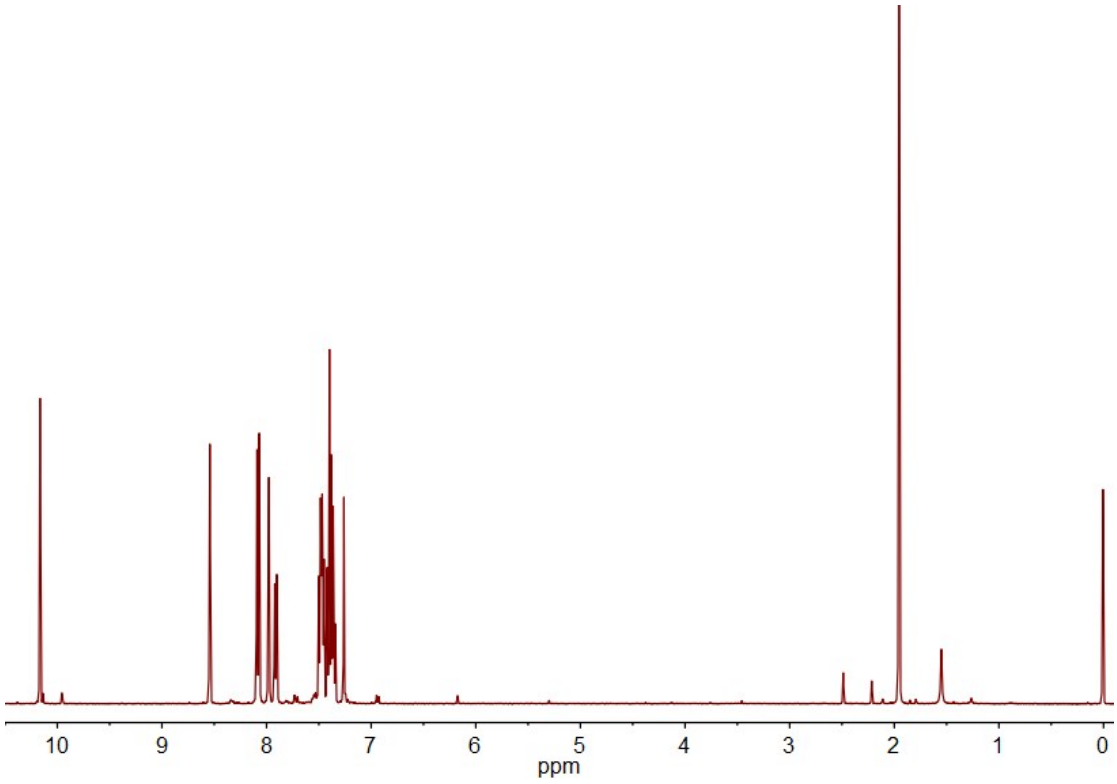

Figure S3. ^{1}H NMR spectrum of **5** ($CDCl_3$, 400 MHz, 298 K)

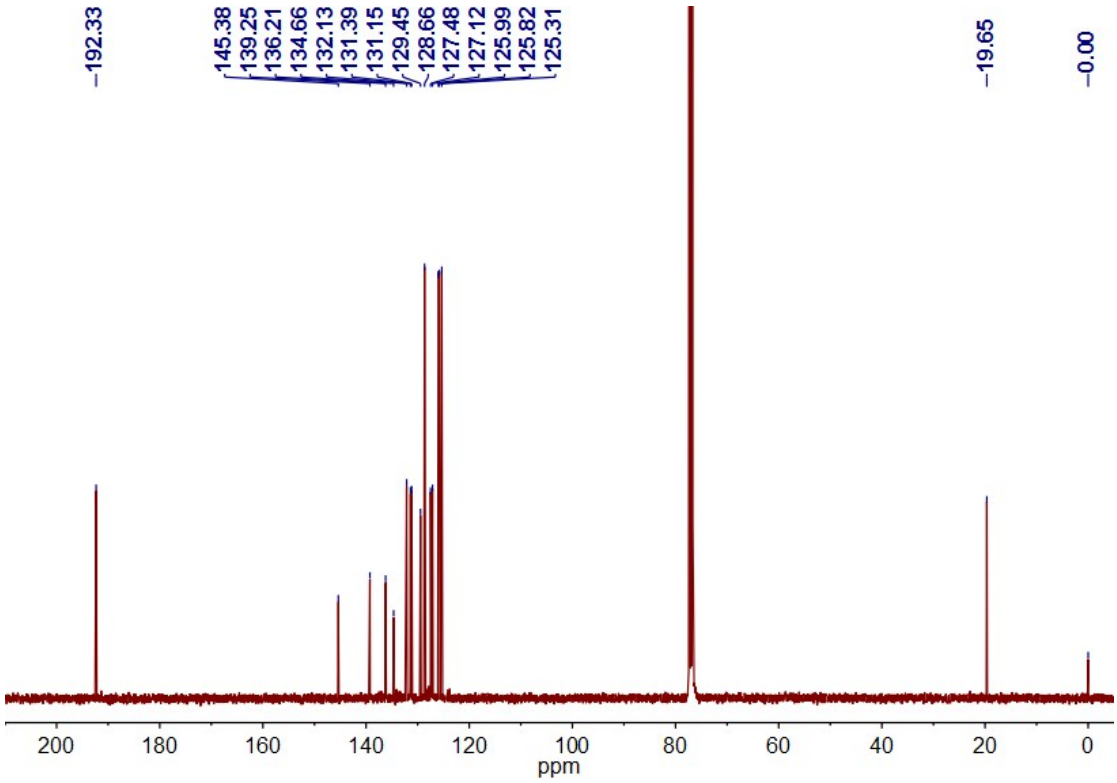

Figure S4. ^{13}C NMR spectrum of **5** ($CDCl_3$, 101 MHz, 298 K)

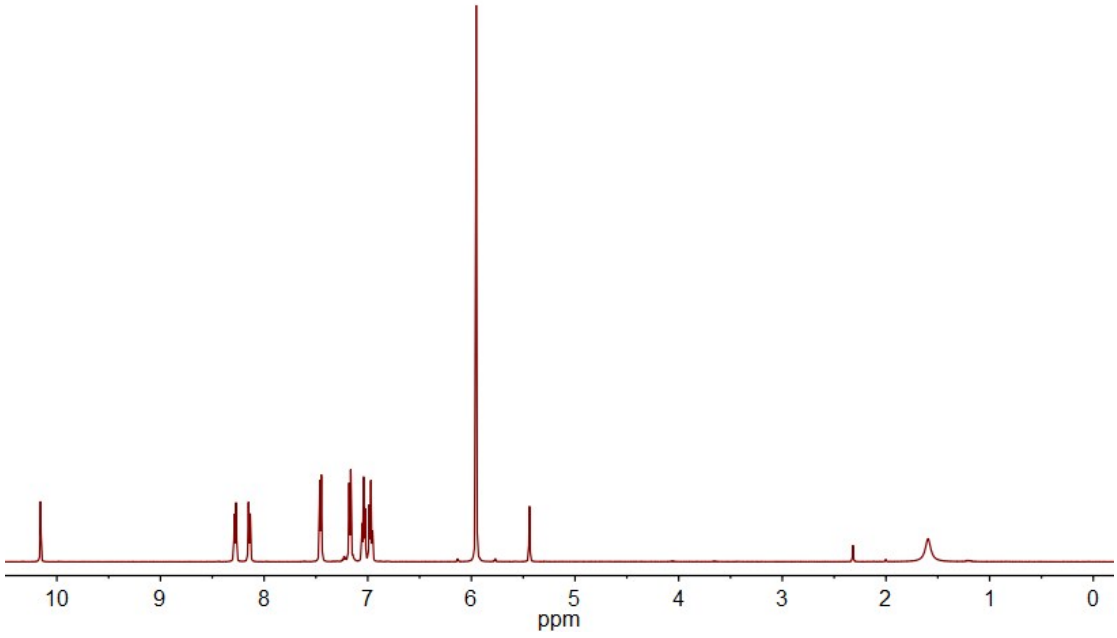

Figure S5. ^{1}H NMR spectrum of **6** ($CDCl_2CDCl_2$, 500 MHz, 298 K)

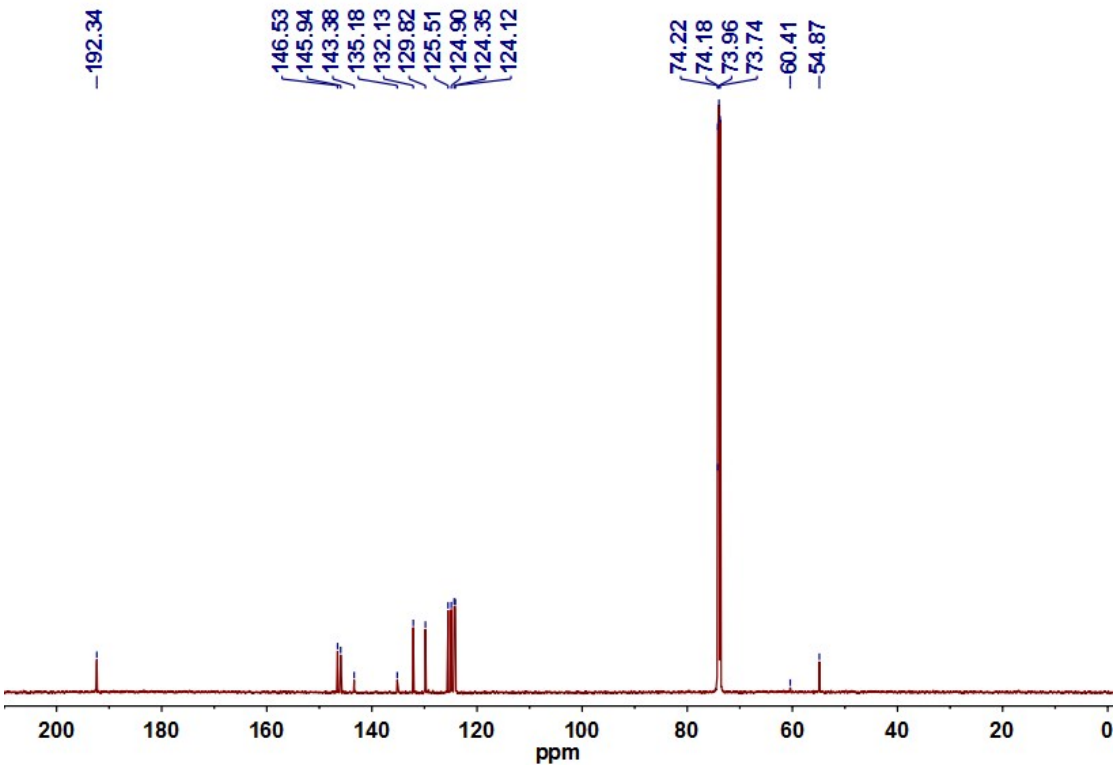

Figure S6. ^{13}C NMR spectrum of **6** ($CDCl_2CDCl_2$, 126 MHz, 298 K)

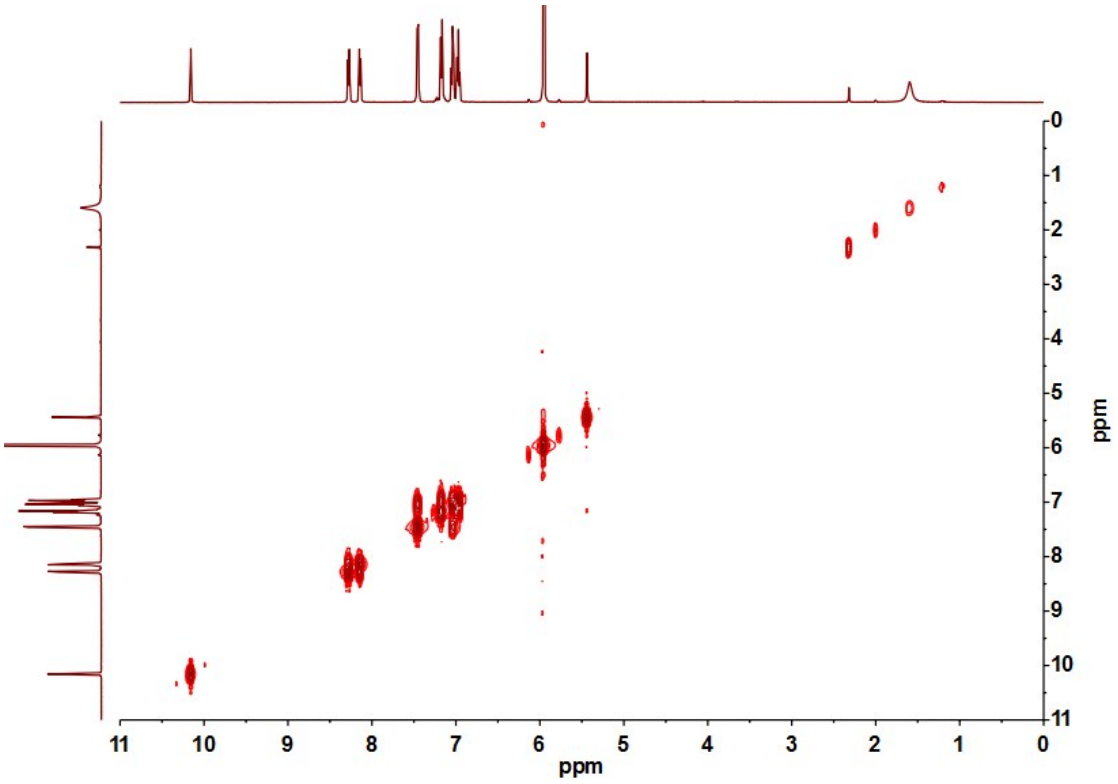

Figure S7. ^{1}H-^{1}H COSY NMR spectrum of **6** ($CDCl_2CDCl_2$, 500 MHz, 298 K)

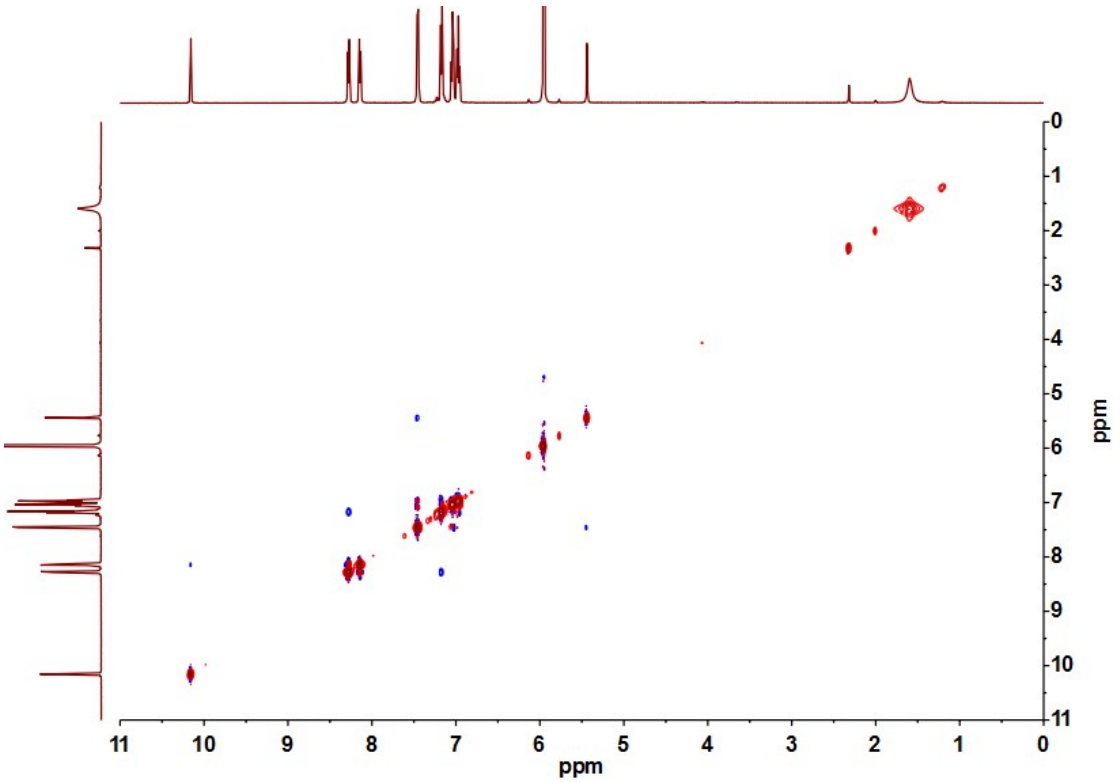

Figure S8. ^{1}H-^{1}H NOESY NMR spectrum of **6** ($CDCl_2CDCl_2$, 500 MHz, 298 K)

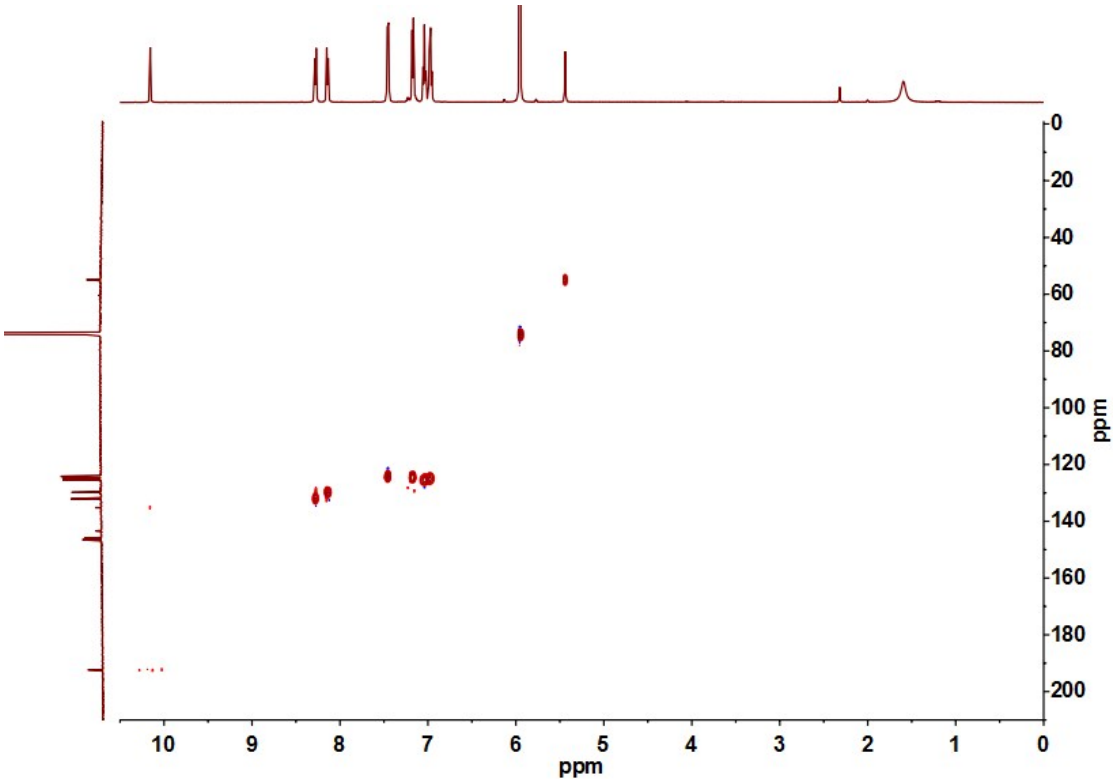

Figure S9. ^{1}H-^{13}C HSQC NMR spectrum of **6** ($CDCl_2CDCl_2$, ^{1}H: 500 MHz, ^{13}C: 126 MHz, 298 K)

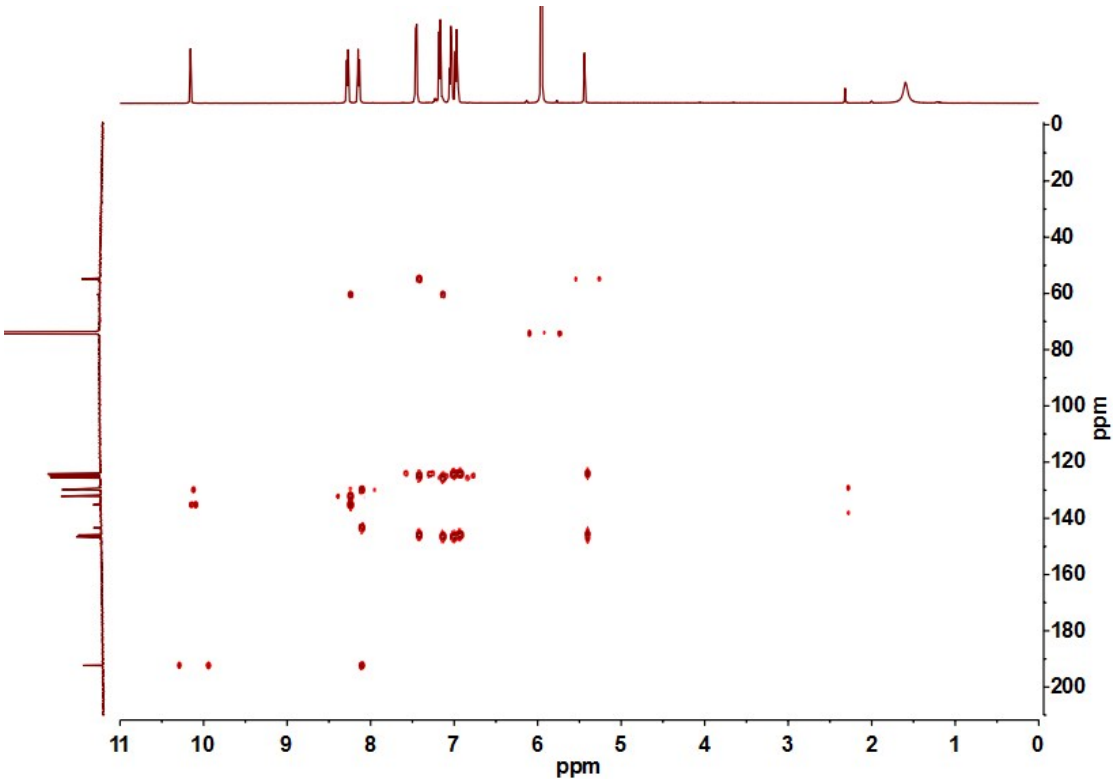

Figure S10. ^{1}H-^{13}C HMBC NMR spectrum of **6** ($CDCl_2CDCl_2$, ^{1}H: 500 MHz, ^{13}C: 126 MHz, 298 K)

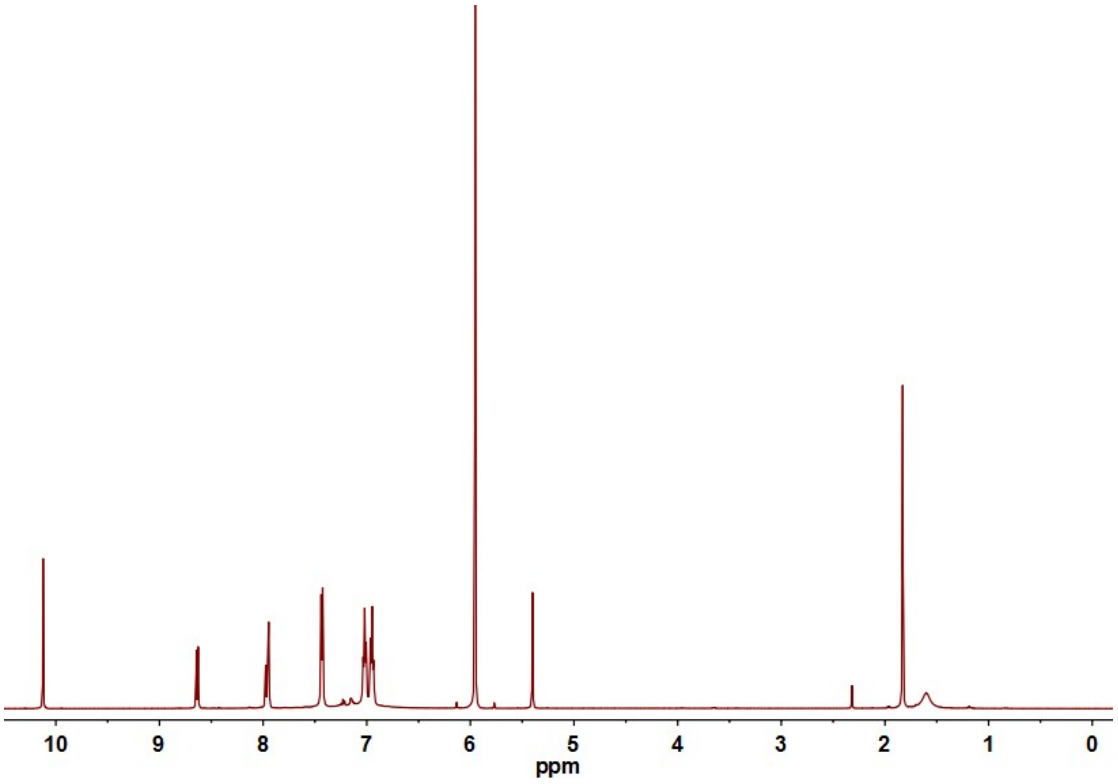

Figure S11. ^{1}H NMR spectrum of **7** ($CDCl_2CDCl_2$, 500 MHz, 298 K)

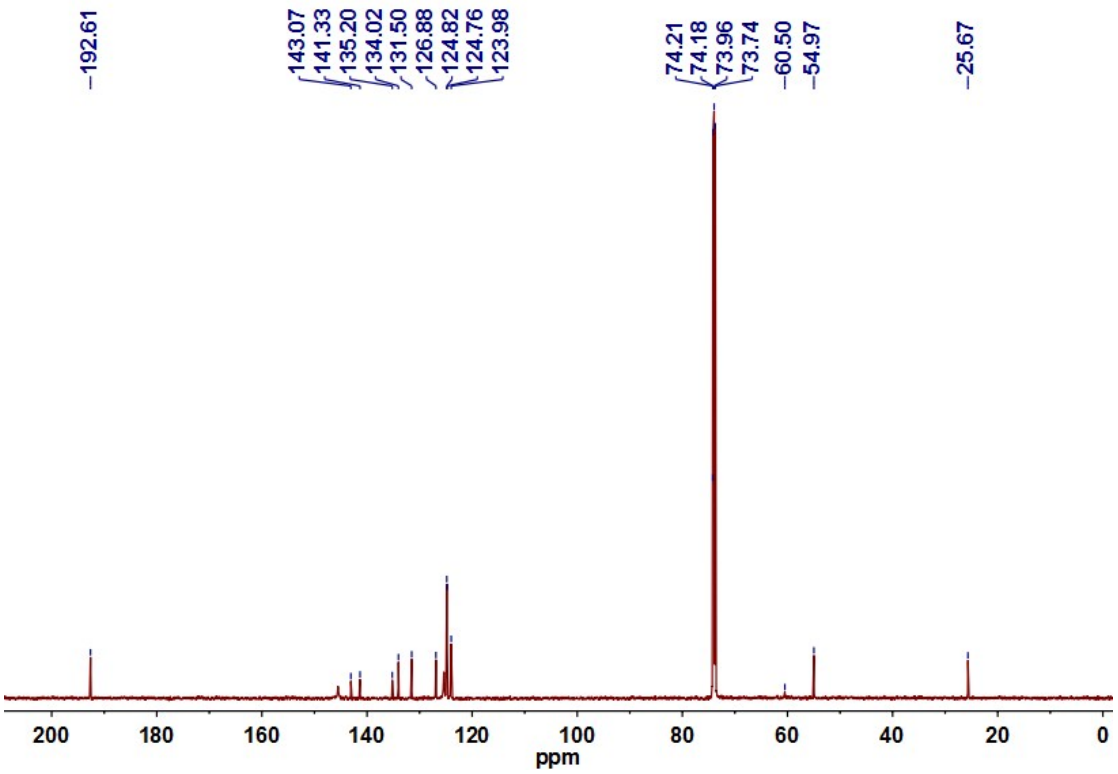

Figure S12. ^{13}C NMR spectrum of **7** ($CDCl_2CDCl_2$, 126 MHz, 298 K)

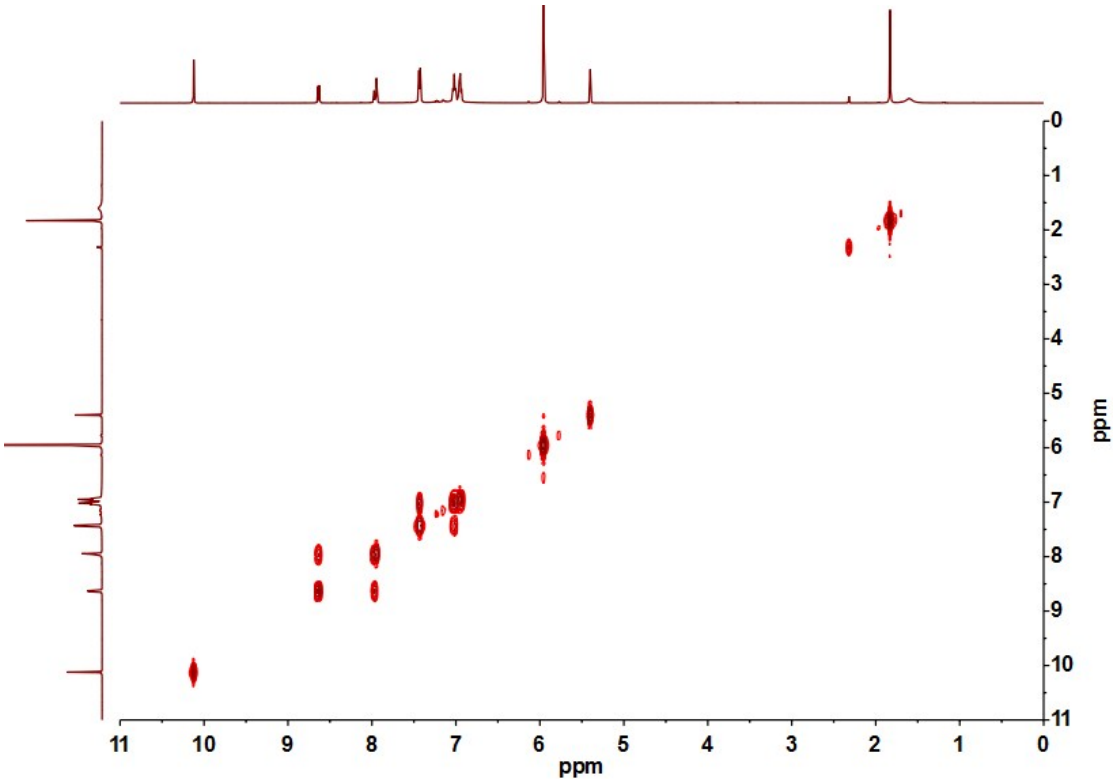

Figure S13. ^{1}H-^{1}H COSY NMR spectrum of **7** ($CDCl_2CDCl_2$, 500 MHz, 298 K)

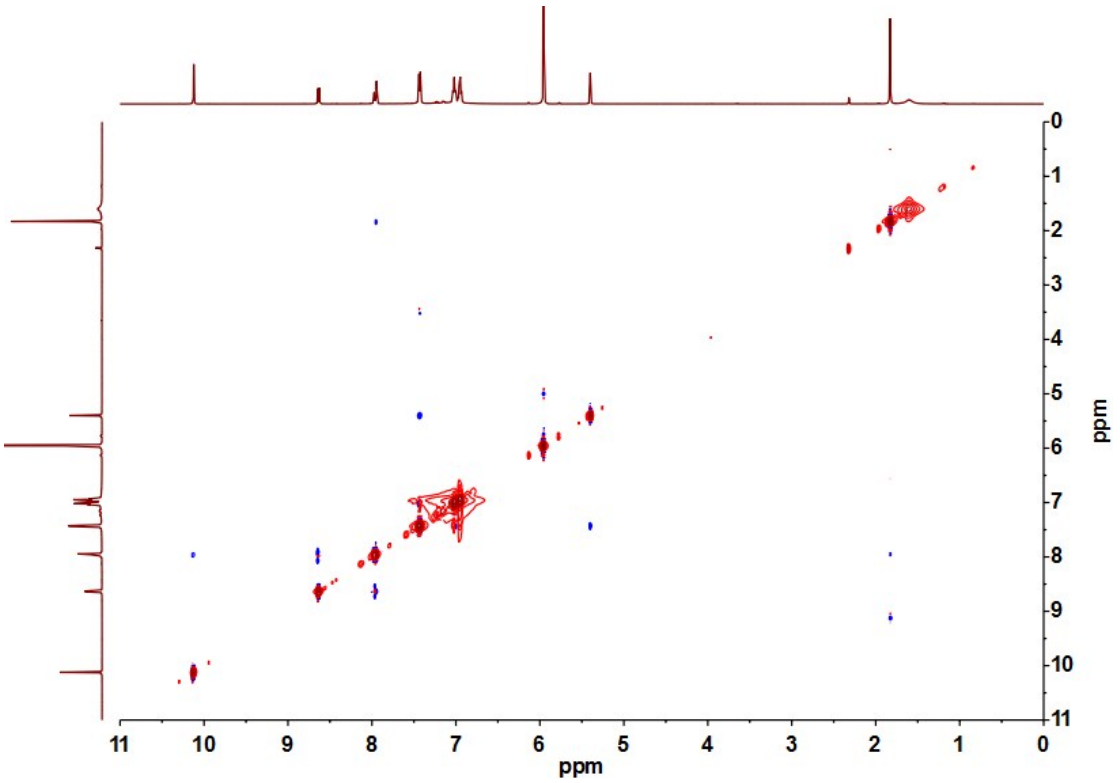

Figure S14. ^{1}H-^{1}H NOESY NMR spectrum of **7** ($CDCl_2CDCl_2$, 500 MHz, 298 K)

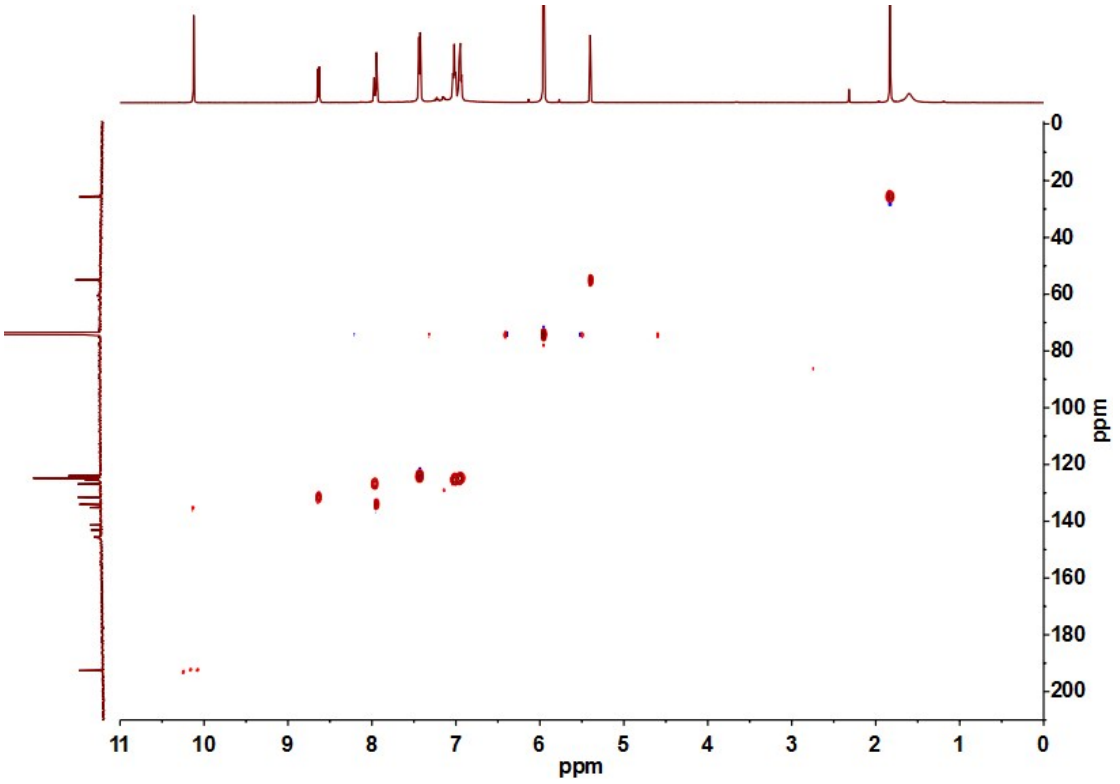

Figure S15. ^{1}H-^{13}C HSQC NMR spectrum of **7** ($CDCl_2CDCl_2$, ^{1}H: 500 MHz, ^{13}C: 126 MHz, 298 K)

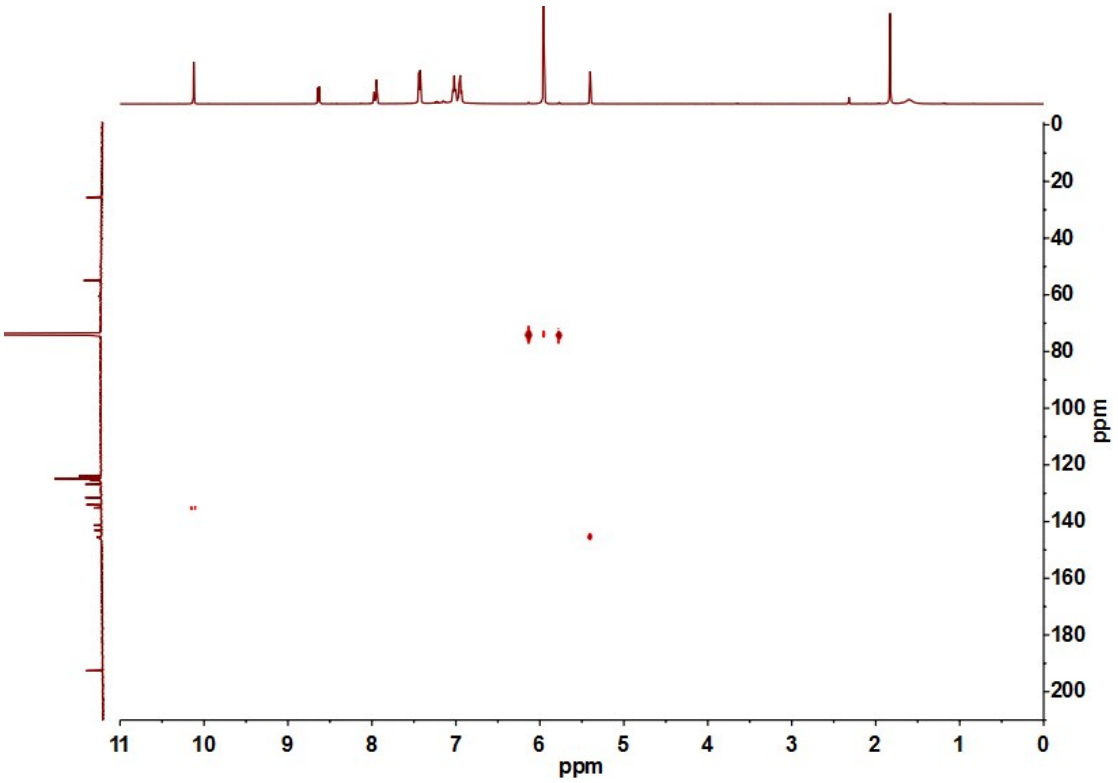

Figure S16. ^{1}H-^{13}C HMBC NMR spectrum of **7** ($CDCl_2CDCl_2$, ^{1}H: 500 MHz, ^{13}C: 126 MHz, 298 K)

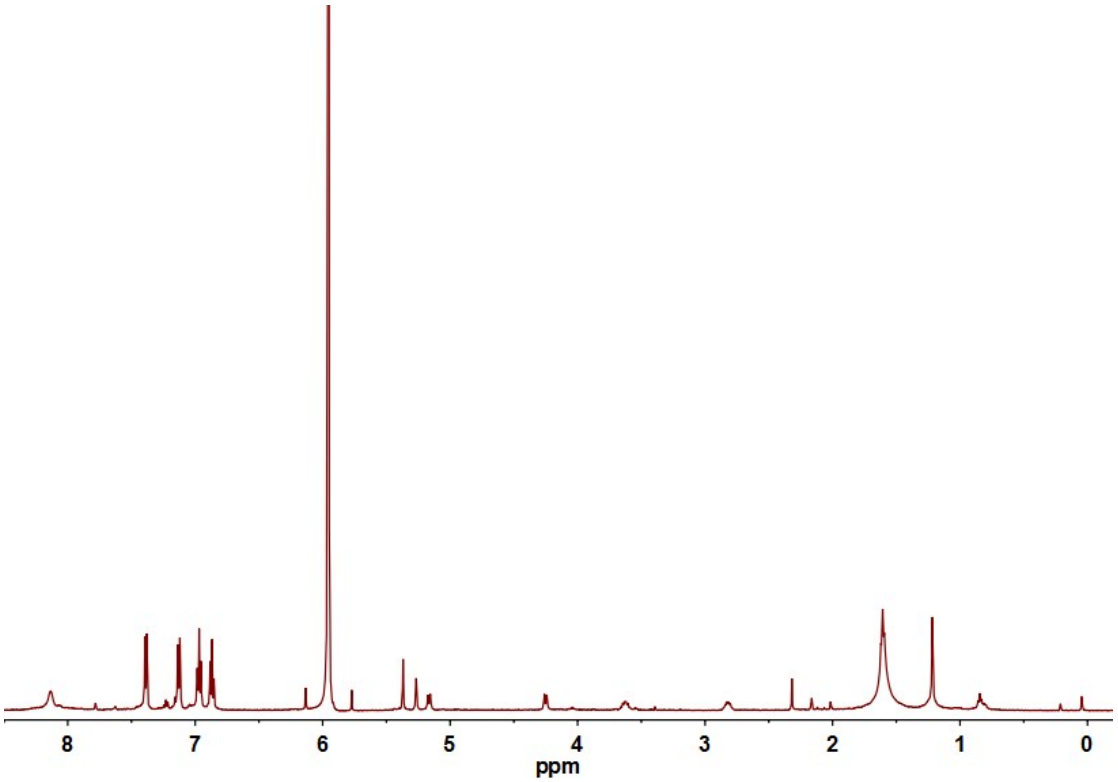

Figure S17. ^{1}H NMR spectrum of **8** ($CDCl_2CDCl_2$, 500 MHz, 298 K)

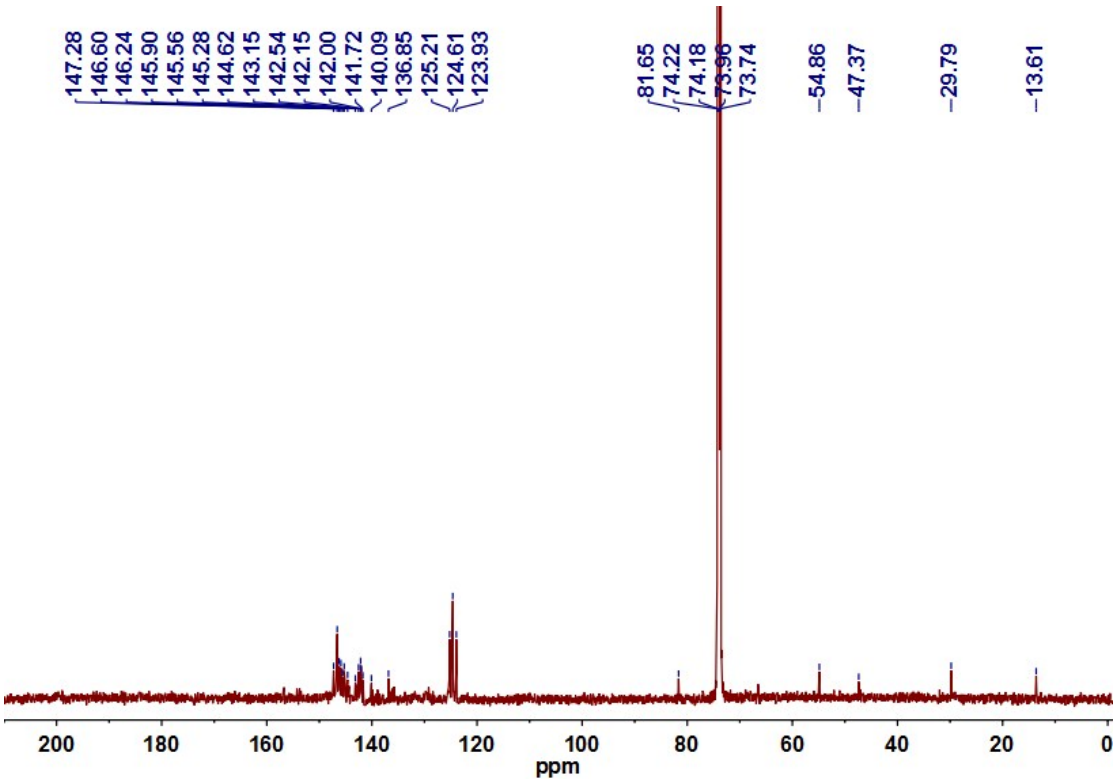

Figure S18. ^{13}C NMR spectrum of **8** ($CDCl_2CDCl_2$, 126 MHz, 298 K)

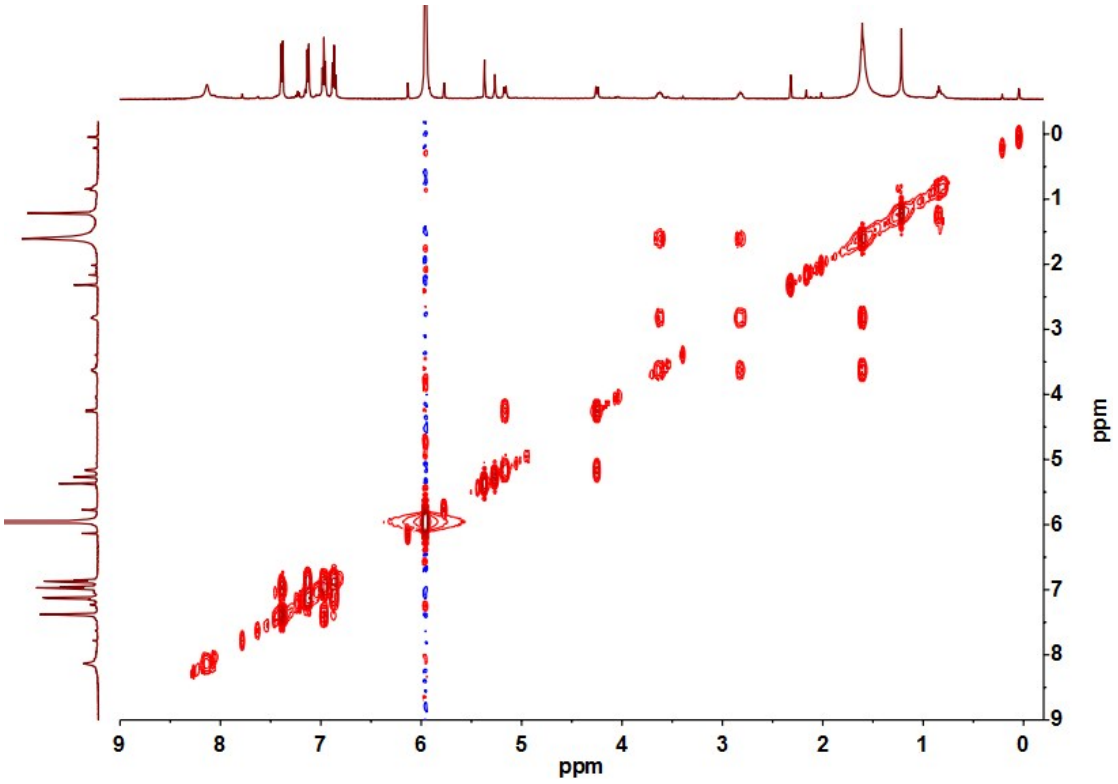

Figure S19. ^{1}H-^{1}H COSY NMR spectrum of **8** ($CDCl_2CDCl_2$, 500 MHz, 298 K)

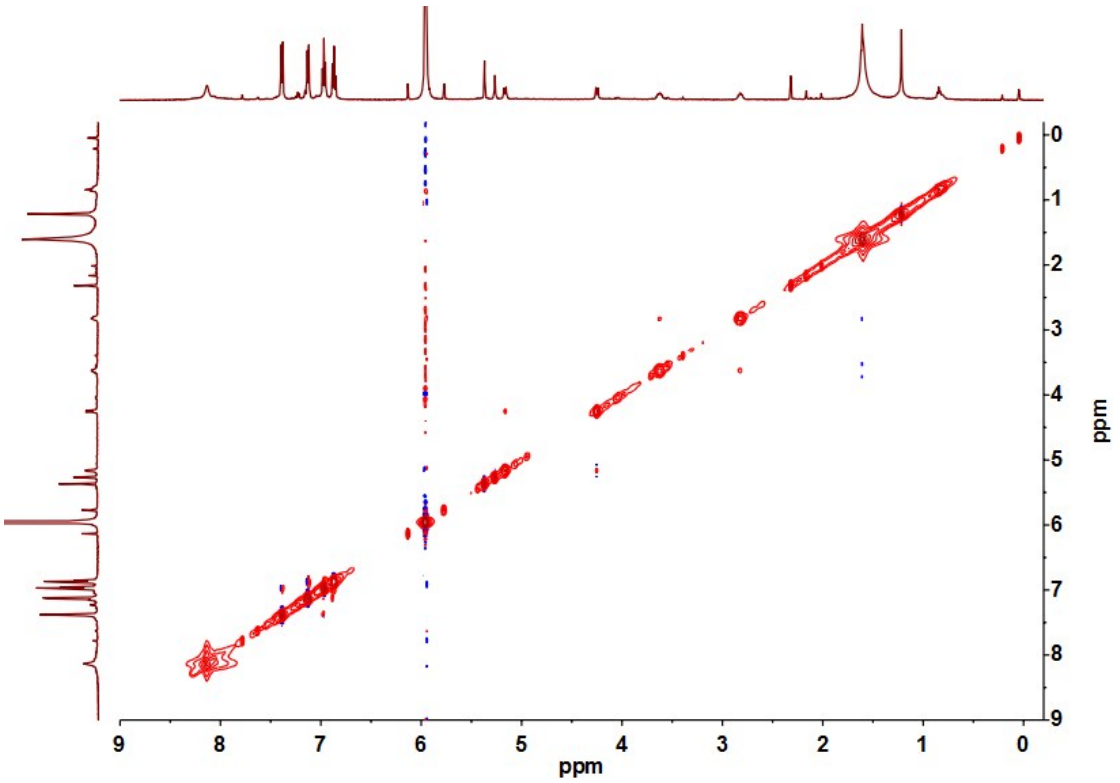

Figure S20. ^{1}H-^{1}H NOESY NMR spectrum of **8** ($CDCl_2CDCl_2$, 500 MHz, 298 K)

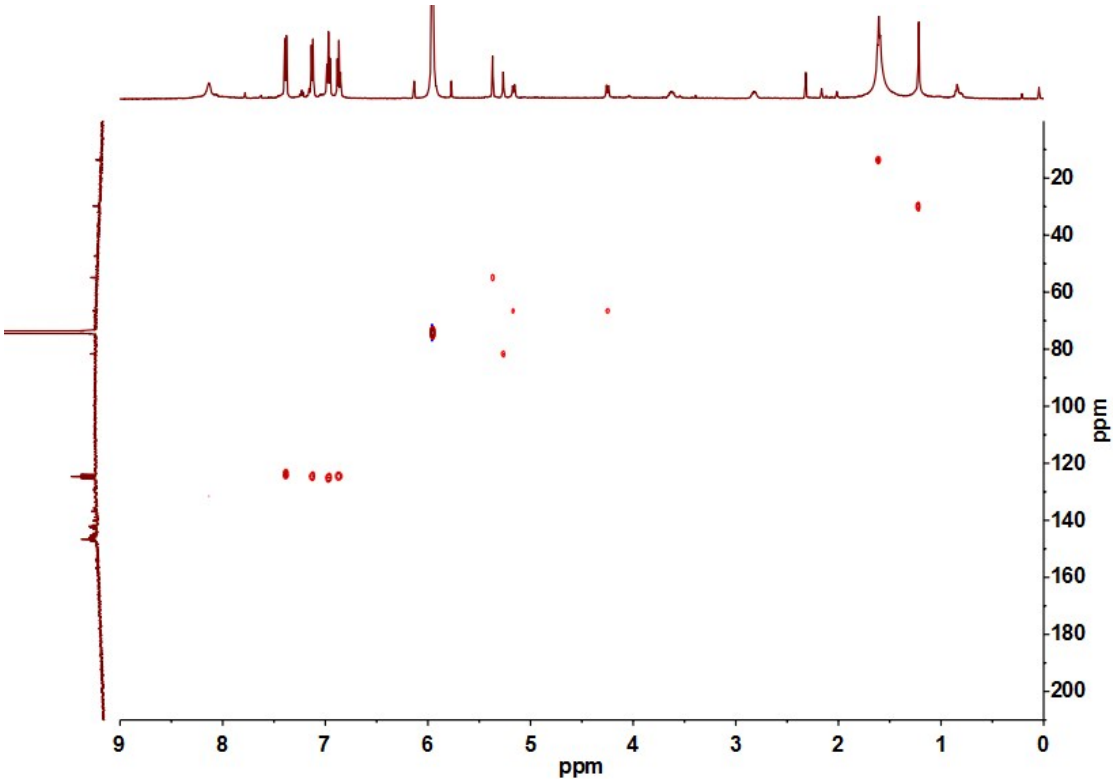

Figure S21. ^{1}H-^{13}C HSQC NMR spectrum of **8** ($CDCl_2CDCl_2$, ^{1}H: 500 MHz, ^{13}C: 126 MHz, 298 K)

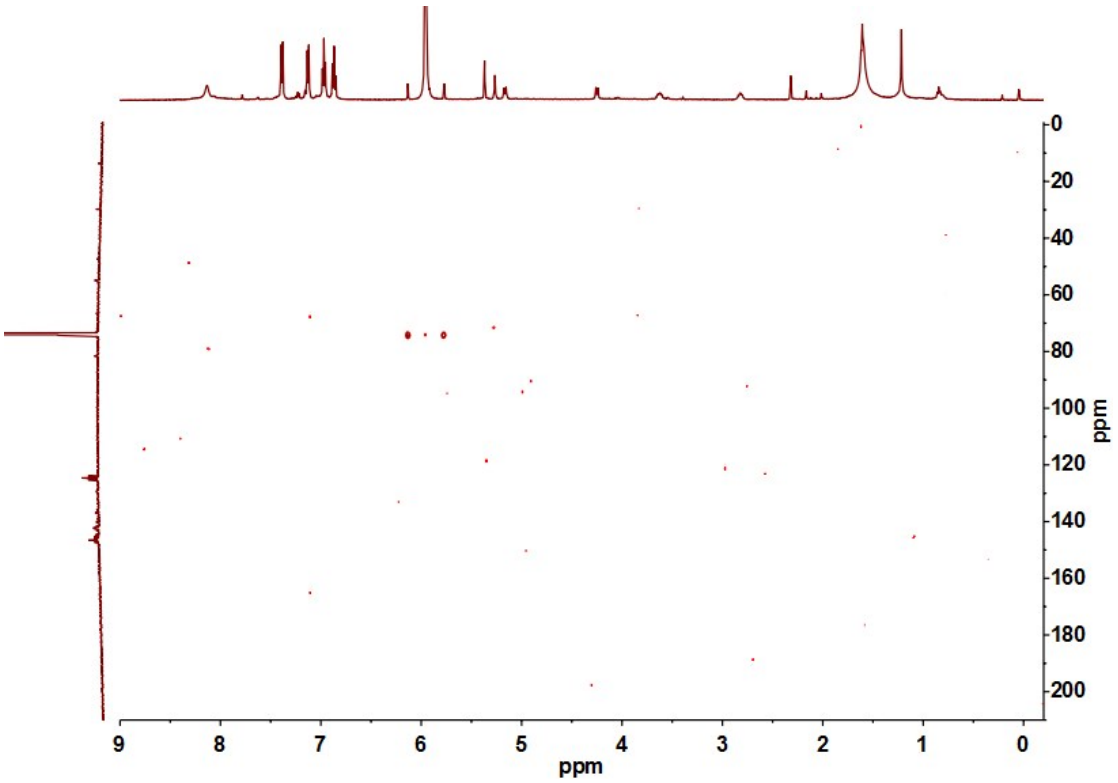

Figure S22. ^{1}H-^{13}C HMBC NMR spectrum of **8** ($CDCl_2CDCl_2$, ^{1}H: 500 MHz, ^{13}C: 126 MHz, 298 K)

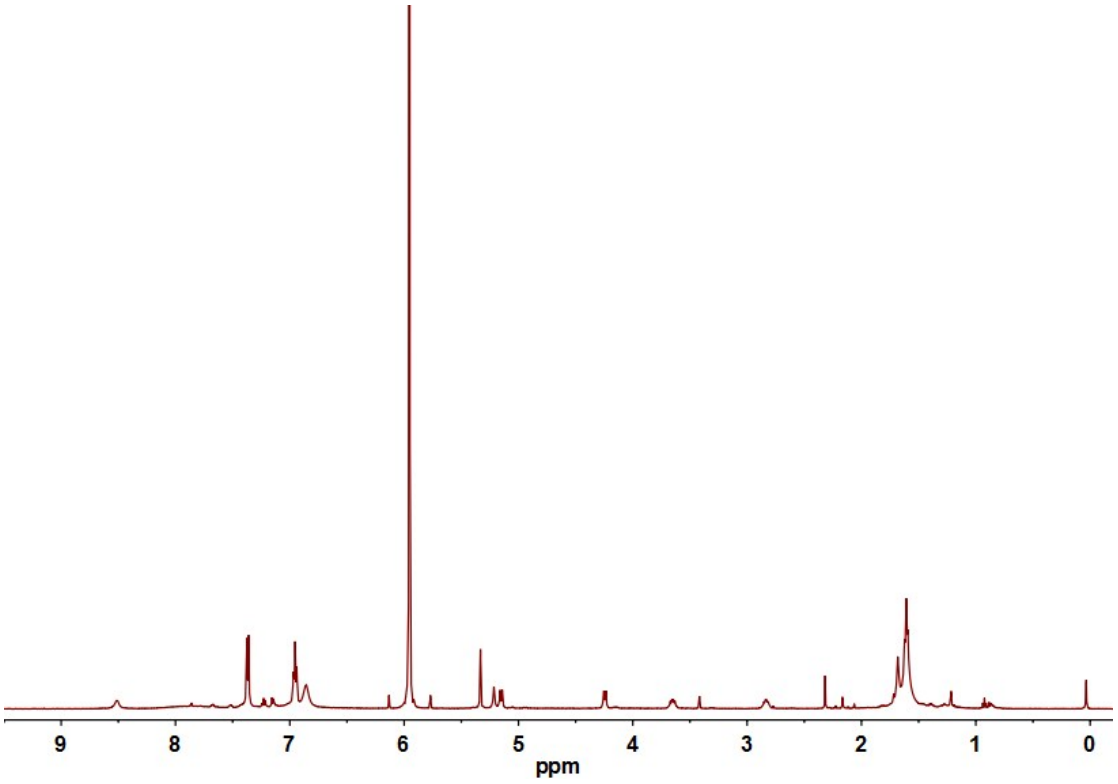

Figure S23. ^{1}H NMR spectrum of **9** ($CDCl_2CDCl_2$, 500 MHz, 298 K)

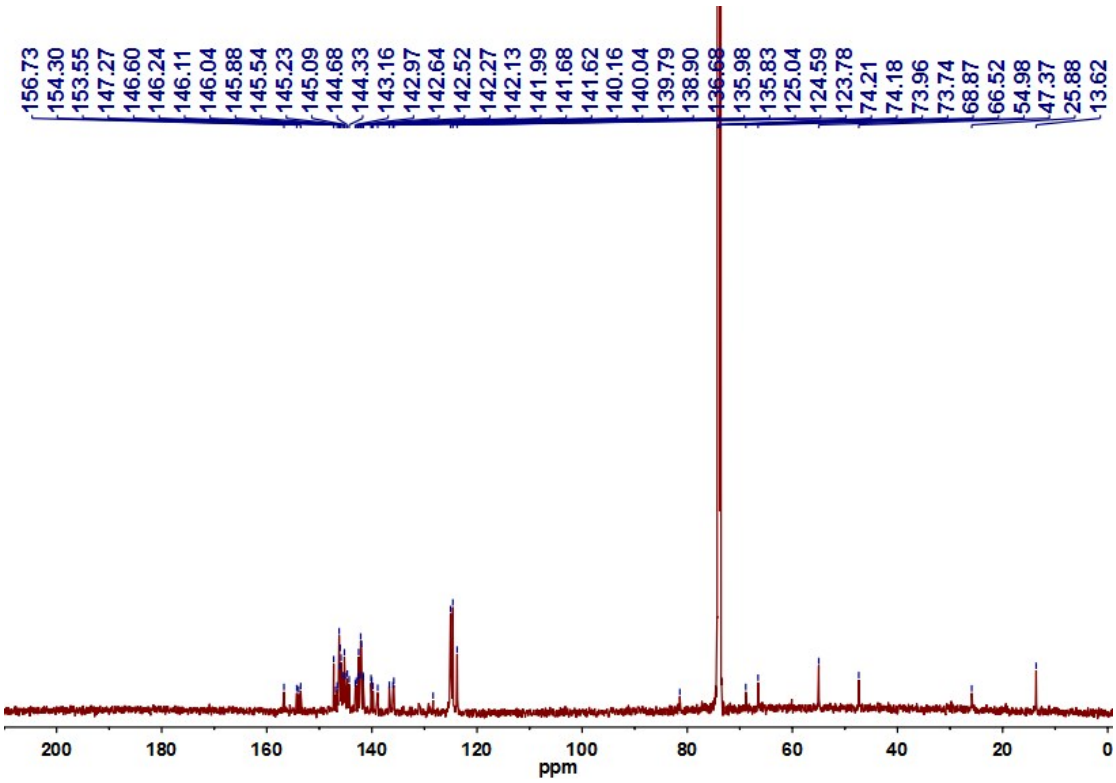

Figure S24. ^{13}C NMR spectrum of **9** ($CDCl_2CDCl_2$, 126 MHz, 298 K)

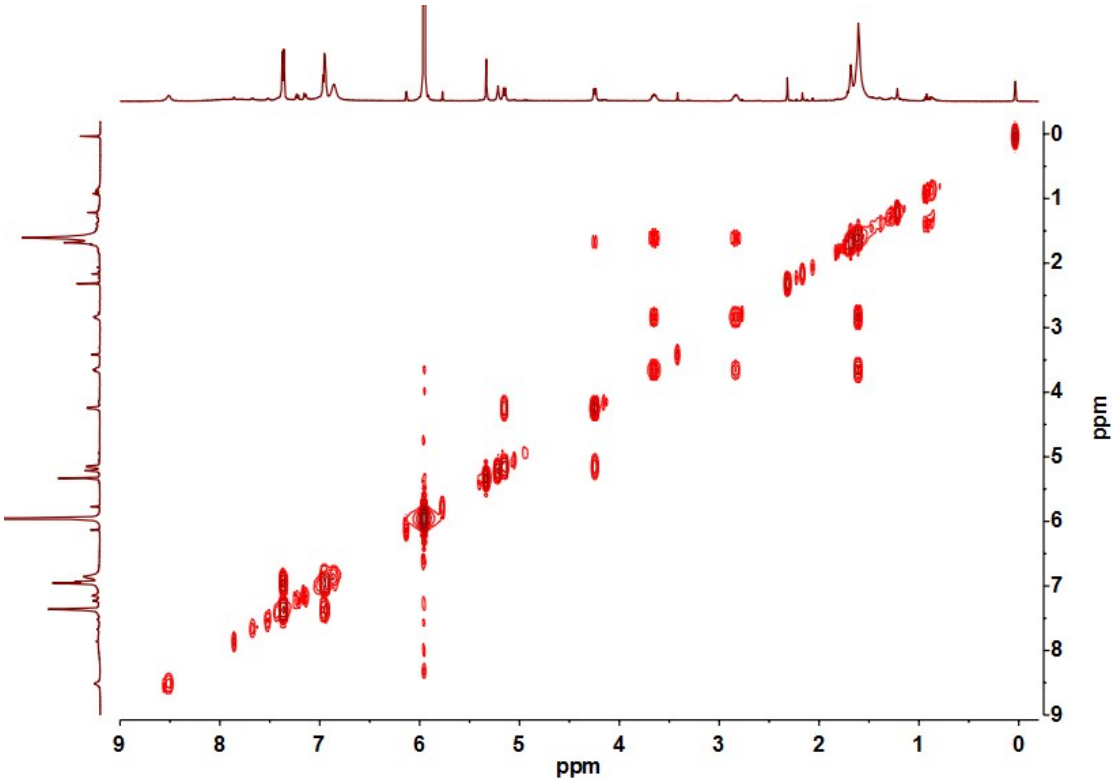

Figure S25. ^{1}H-^{1}H COSY NMR spectrum of **9** ($CDCl_2CDCl_2$, 500 MHz, 298 K)

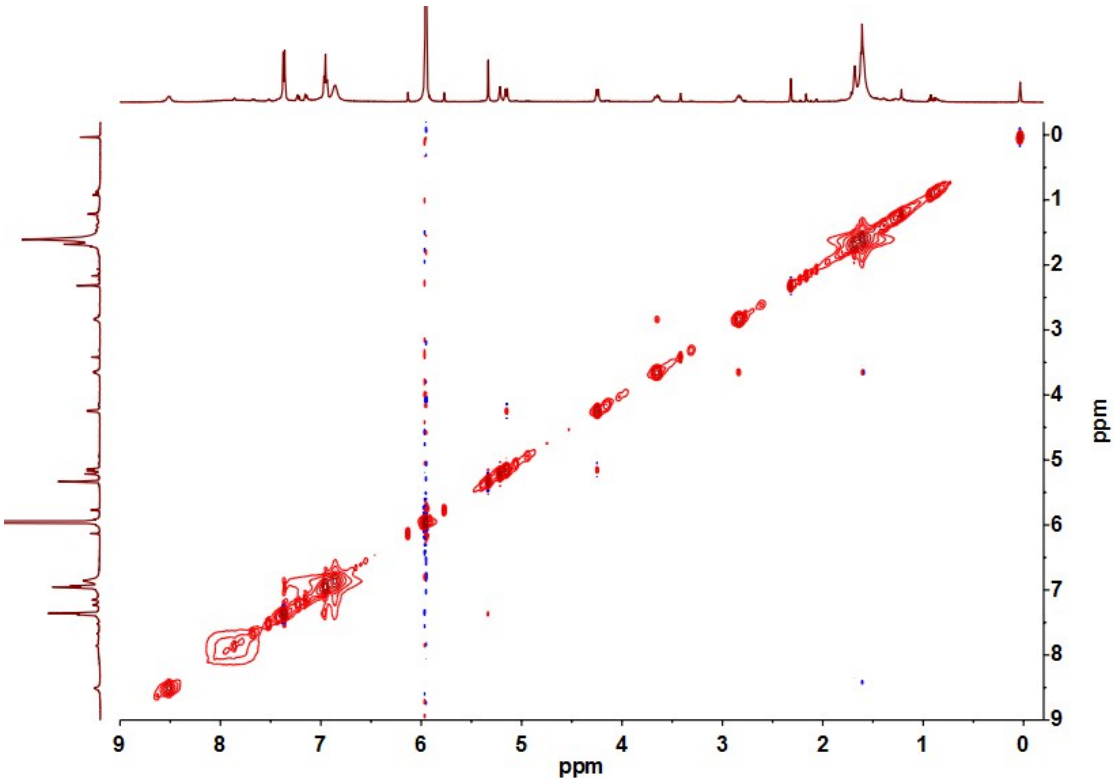

Figure S26. ^{1}H-^{1}H NOESY NMR spectrum of **9** ($CDCl_2CDCl_2$, 500 MHz, 298 K)

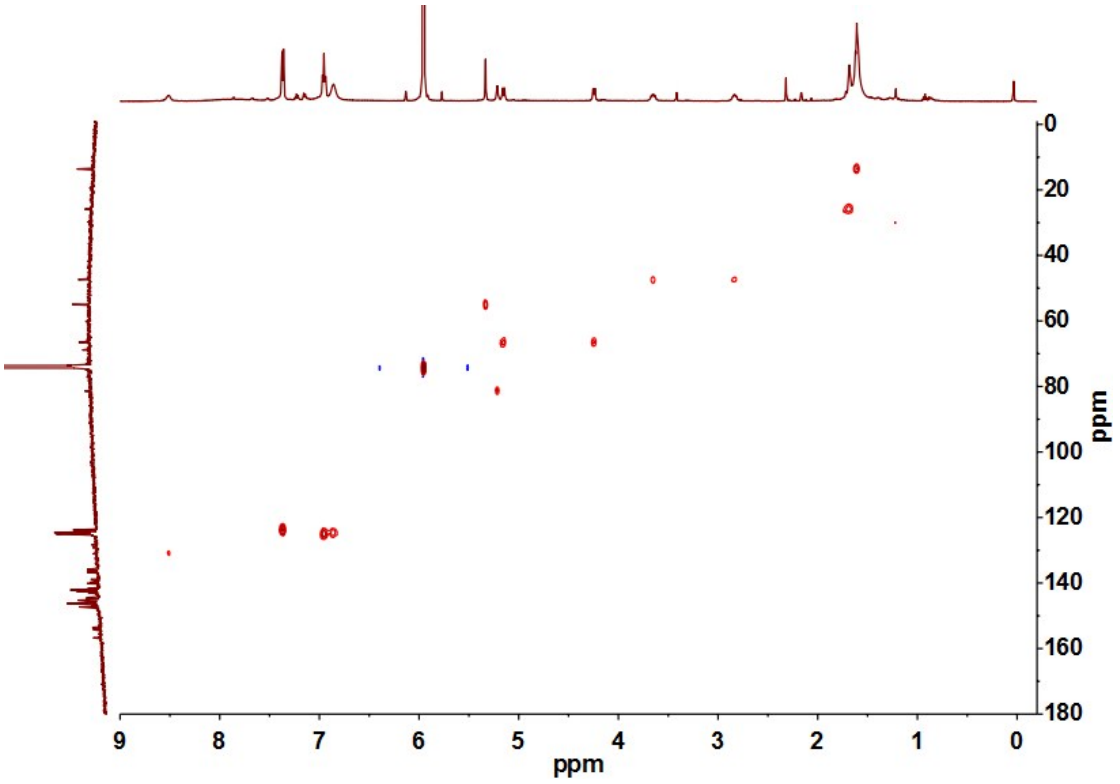

Figure S27. ^{1}H-^{13}C HSQC NMR spectrum of **9** ($CDCl_2CDCl_2$, ^{1}H: 500 MHz, ^{13}C: 126 MHz, 298 K)

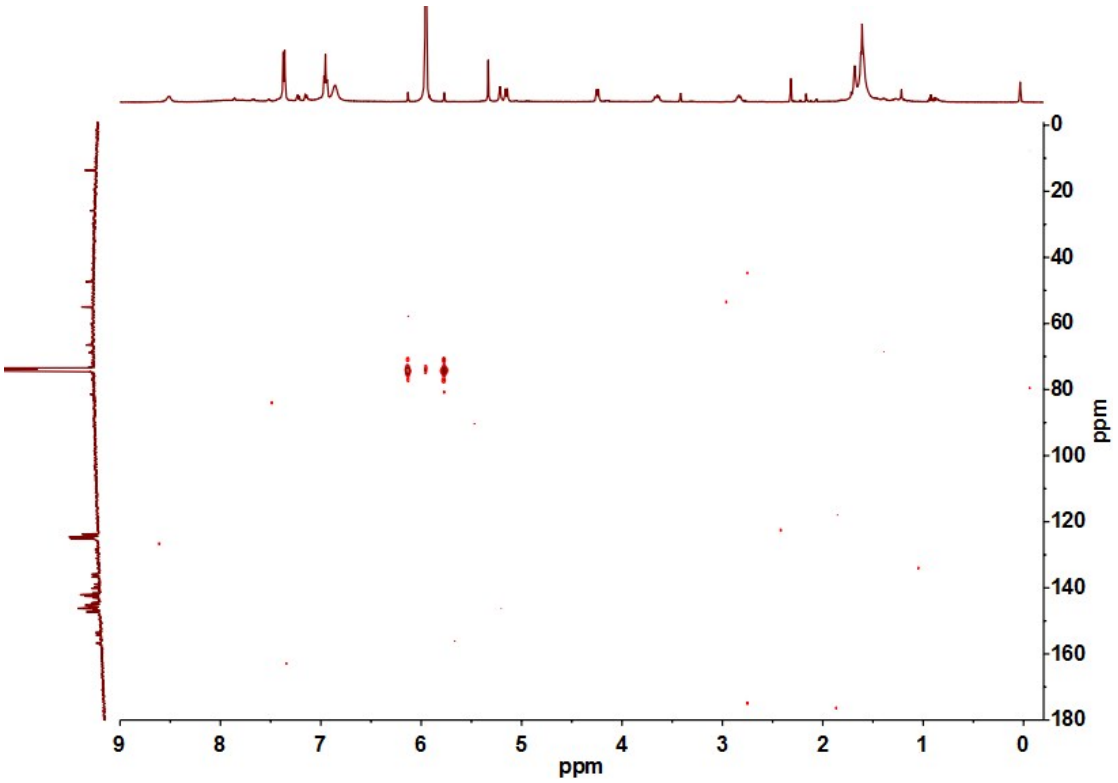

Figure S28. ^{1}H-^{13}C HMBC NMR spectrum of **9** ($CDCl_2CDCl_2$, ^{1}H: 500 MHz, ^{13}C: 126 MHz, 298 K)

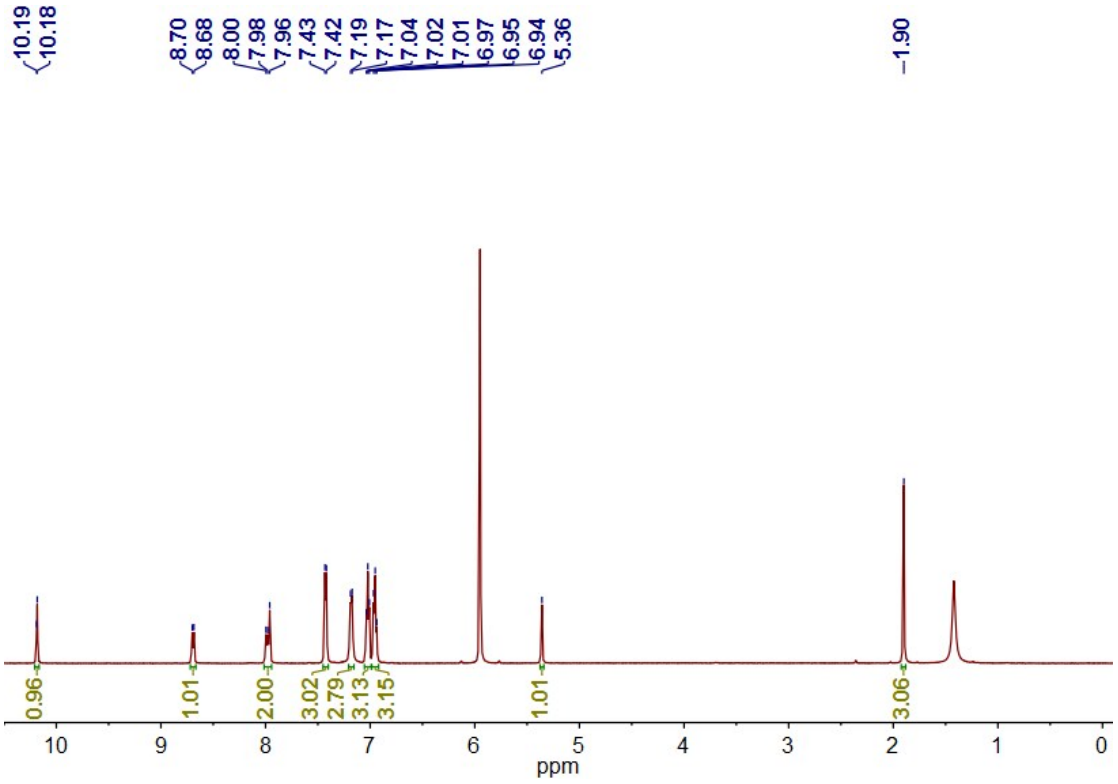

Figure S29. ^{1}H NMR spectrum of **7** ($CDCl_2CDCl_2$, 500 MHz, 378 K)

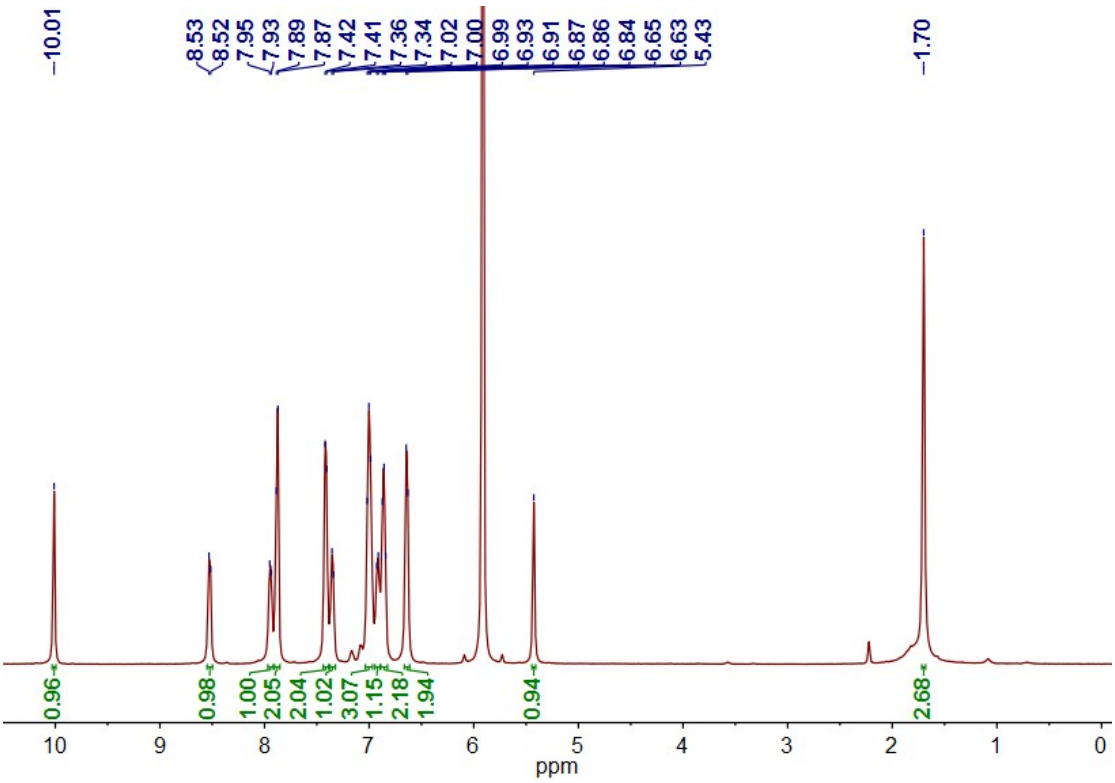

Figure S30. ^{1}H NMR spectrum of **7** ($CDCl_2CDCl_2$, 500 MHz, 238 K)

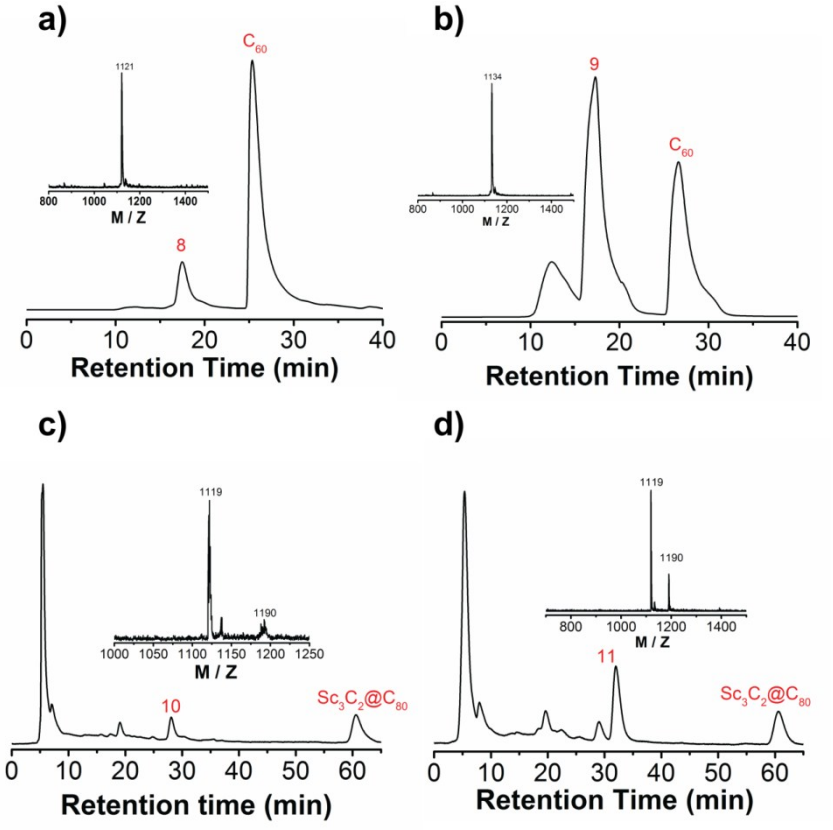

Figure S31. Chromatograms of the isolated **8** (a), **9** (b), **10** (c) and **11** (d) (20×250 mm Buckyprep colum, flow rate 6 mL/min for **8** and **9**, 12 mL/min for **10** and **11**. toluene as eluent). The insets show the MALDI-TOF-MS profiles of **8**, **9**, **10** and **11**, respectively.

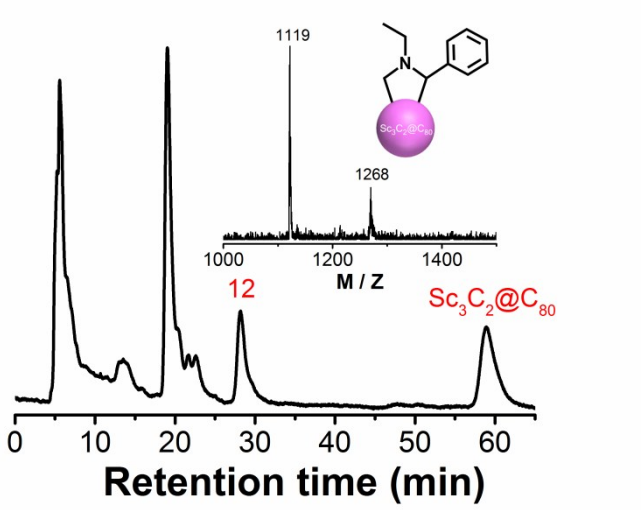

Figure S32. Chromatogram of the isolated **12** (20×250 mm Buckyprep colum, flow rate 12 mL/min. toluene as eluent). The insets show the MALDI-TOF-MS profiles and molecular structure of **12**.

Assignments of ^{1}H-NMR protons of the triptycene parts for 6, 7, 8 and 9

The assignments of ^{1}H-NMR protons for 6, 7, 8 and 9 were confirmed by their ^{1}H, ^{13}C, ^{1}H-^{1}H COSY, ^{1}H-^{1}H NOESY, ^{1}H-^{13}C HSQC and ^{1}H-^{13}C HMBC NMR spectra.

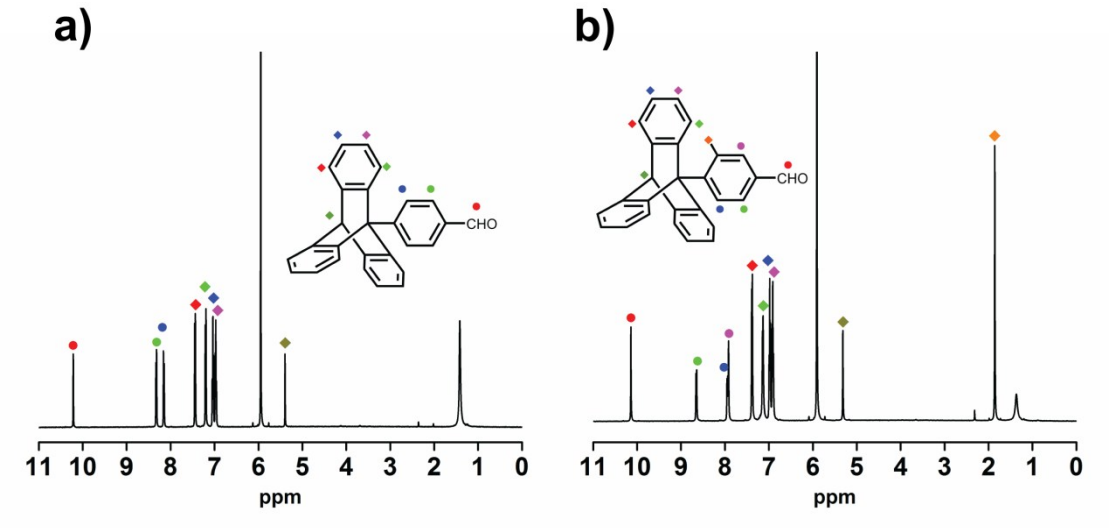

Figure S33. The assignments of ^{1}H-NMR protons of **6** (a) at 298 K and **7** (b) at 378 K. The different colors of squares and circles in the ^{1}H-NMR spectra indicate the corresponding protons of the molecules. The ^{1}H-NMR spectrum at 378 K for **7** was chosen due to its high coalescence temperature.

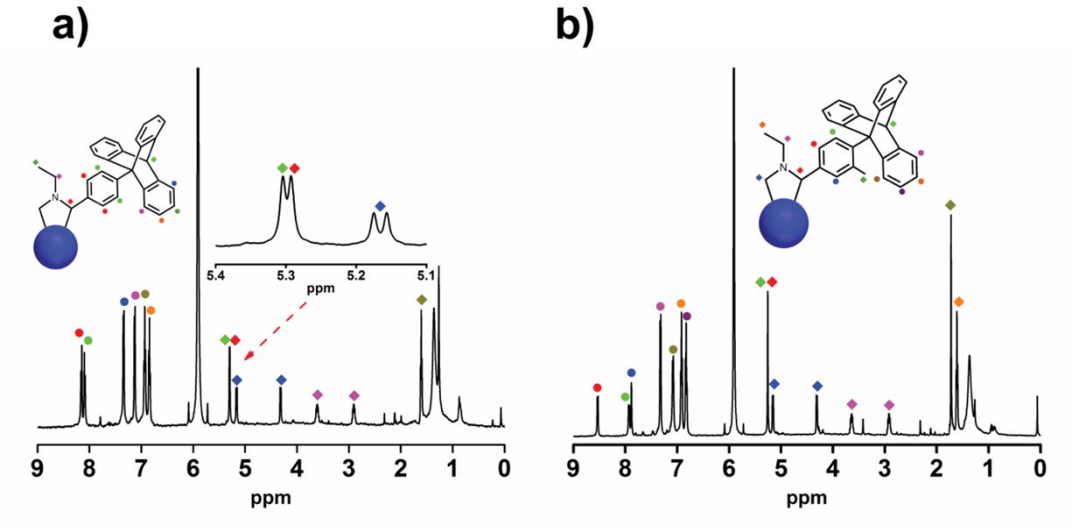

Figure S34. The assignments of ^{1}H-NMR protons of **8** (a) at 298 K and **9** (b) at 378 K. The different colors of squares and circles in the ^{1}H-NMR spectra indicate the corresponding protons of the molecules. The ^{1}H-NMR spectrum at 378 K for **9** was chosen due to its high coalescence temperature.

VT-^{1}H NMR experiments of 6, 7, 8 and 9

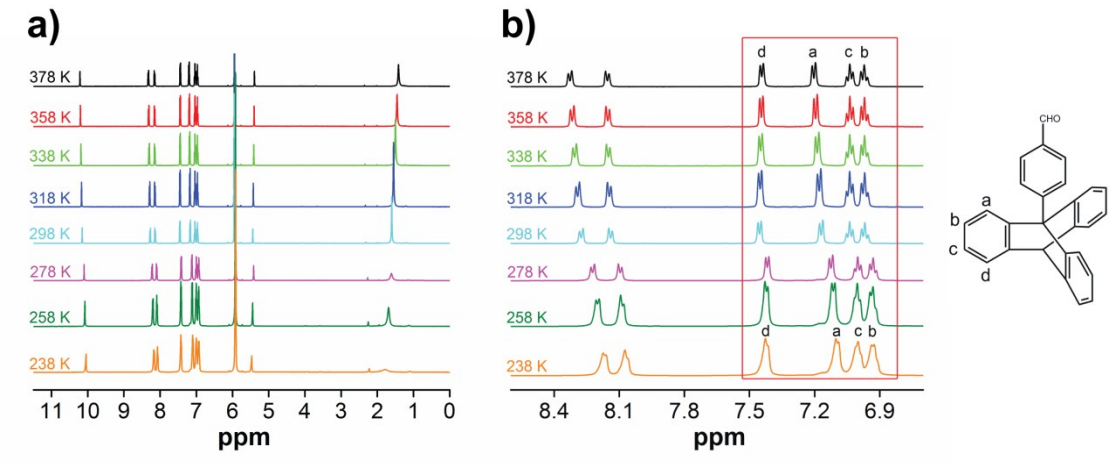

Figure S35. Variable temperature-^{1}H NMR (VT-^{1}H NMR) spectra of **6** (a) and partial VT-^{1}H NMR spectra of **6** (b) (^{1}H NMR, $CDCl_2CDCl_2$, 500 MHz). The signals of the triptycene parts of **6** are shown in red square and the right structural formula illustrates the only one set of protons for the phenylene rings.

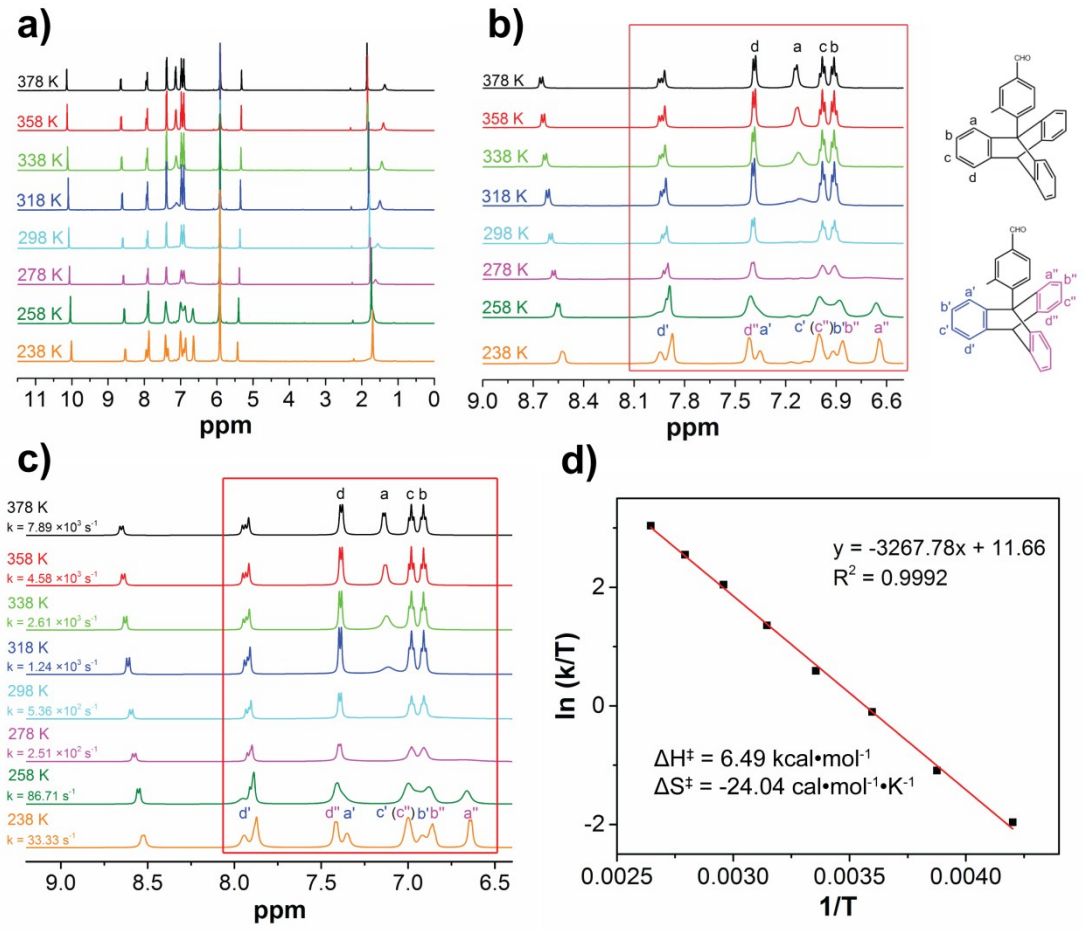

Figure S36. Variable temperature-^{1}H NMR (VT-^{1}H NMR) spectra of **7** (a) and partial VT-^{1}H NMR spectra of **7** (b) (^{1}H NMR, $CDCl_2CDCl_2$, 500 MHz). The simulated spectra were calculated with DNMR Line Shape Analysis procedure implemented in the Topspin 2.1 program with the two-state exchange model (c). The Eyring plots calculated from simulated spectra (d). The signals of the triptycene parts of **7** are shown in the red squares and the structural formulas illustrate the splits of protons for the phenylene rings of **7** with decreasing temperature.

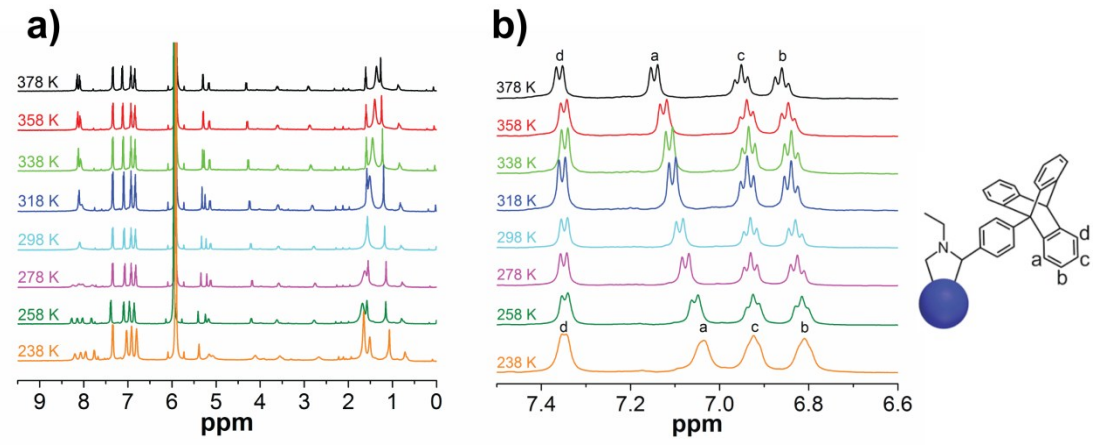

Figure S37. Variable temperature-^{1}H NMR (VT-^{1}H NMR) spectra of **8** (a) and VT-^{1}H NMR spectra of the phenylene rings for **8** (b) (^{1}H NMR, $CDCl_2CDCl_2$, 500 MHz). The right structural formula illustrates only one set of the protons for the phenylene rings.

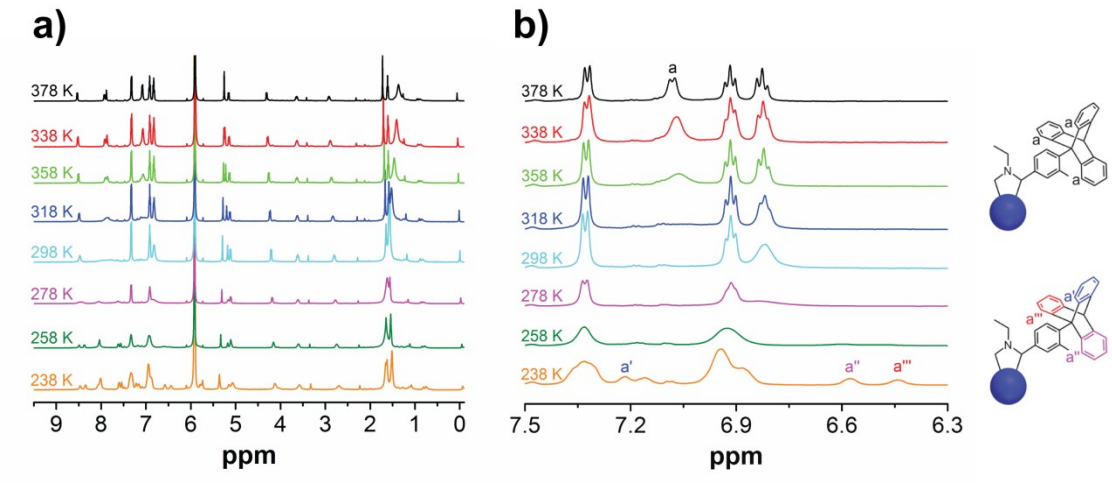

Figure S38. Variable temperature-^{1}H NMR (VT-^{1}H NMR) spectra of **9** (a) and VT-^{1}H NMR spectra of the phenylene rings for **9** (b) (^{1}H NMR, $CDCl_2CDCl_2$, 500 MHz). The right structural formulas illustrate the splits of protons for the phenylene rings of **9** with decreasing temperature.

EPR measurements and analyses of 10, 11 and 12

The EPR spectra of compound **10**, **11 and 12** at different temperatures were measured in situ on Bruker E500 with continues-wave X band frequency (~9.5 GHz). For all the measurements of EPR spectra, the concentration of **10** (0.04 M) in toluene was the same as that of **11 and 12**. Before the measurements, the samples were degassed for three times to avoid the oxygen.

The signal intensity is the peak to peak height (the maximum difference of positive values and negative values) in the EPR spectra.[4]

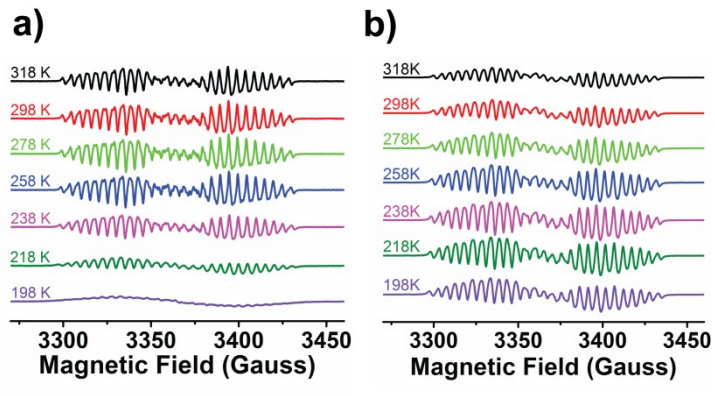

Figure S39. Variable temperature-EPR (VT-EPR) spectra of **11** (left) and **12** (right).

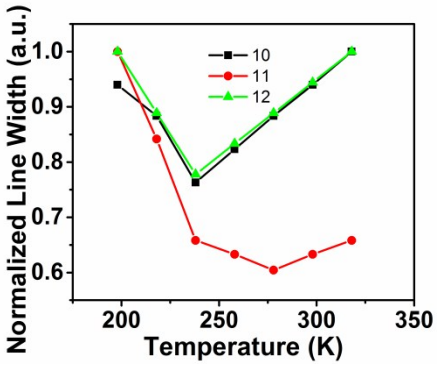

Figure S40. Normalized line widths of EPR spectra for **10**, **11** and **12** at different temperatures.

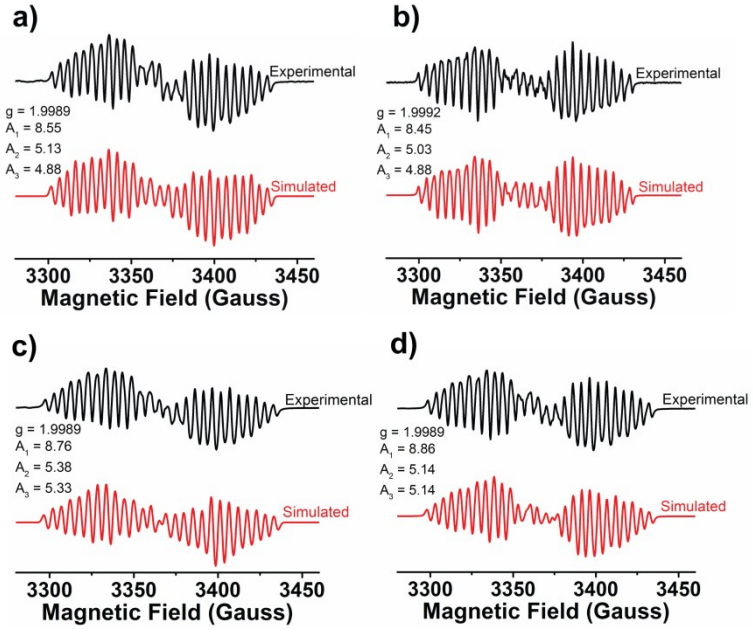

Figure S41. The experimental (black) and simulated (red) EPR spectra of **10** (a) and **11** (b) at 318 K and the experimental (black) and simulated (red) EPR spectra of **12** at 318 K (c) and 238 K (d). The resultant g and hyperfine coupling tensors are listed for each trace.

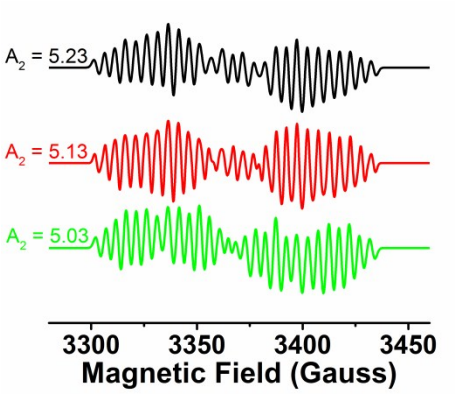

Figure S42. The simulated EPR spectra through changing the hyperfine coupling constant A_2 from 5.23G-5.03G (g = 1.9989; A_1 = 8.55; A_3 = 4.88). The small variation of the couplings (within 0.1 G) can obviously influence the simulated spectra. So the difference of 0.1-0.2G is indeed meaningful and can illustrate the changes of paramagnetic peoperties.

References

1 H. Shinohara, M. Inakuma, N. Hayashi, H. Sato, Y. Saito, T. Kato and S. Bandow, *J. Phys. Chem.*, 1994, **98**, 8597-8599.

2 T. Wang, J. Wu, W. Xu, J. Xiang, X. Lu, B. Li, L. Jiang, C. Shu and C. Wang, *Angew. Chem. Int. Ed.*, 2010, **49**, 1786-1789.

3 S. Stoll and A. Schweiger, *J. Magn. Reson.*, 2006, **178**, 42-55.

4 H. Meng, C. Zhao, Y. Li, M. Nie, C. Wang and T. Wang, *Nanoscale*, 2018, **10**, 3291-3298.